LAWRENCE
LIVERMORE
NATIONAL
LABORATORY

KDFOC3:

A Nuclear Fallout

Assessment Capability

T. Harvey
F. Serduke
L. Edwards
L. Peters

1992

DISCLAIMER

The KDFOC3 Fallout Model

KDFOC3 predicts the groundshine gamma doses from deposited fission debris and areal deposition of individual radionuclides. It develops nuclear debris parcels that follow trajectories defined by the winds, turbulent diffusion, and gravitational settling. When the parcels hit the ground, their activity is summed to yield overall fallout patterns. KDFOC3 is a so-called "disk-tosser" designed to handle a measured wind sounding. Other attributes are that it: conserves radioactivity; has an empirical stem cloud; uses SMALL BOY activity-particle sizes for surface bursts; and, has a continuous, adjustable activity-height distribution from the top of the main cloud to the ground. KDFOC3 has been developed at LLNL as an "in-house" tool to assess single-burst scenarios for real and hypothetical nuclear devices. The model is continuous in all physical parameters, both as a function of depth of burial and of variations in specified winds. KDFOC's success as a mode was tested by the model's overall fit to NTS data where it achieved an agreement to measured patterns to a standard deviation of about 40%. Its results have been compared with small yield nuclear shots, especially Little Feller II. The results agreed better than those of other models, and in all but one case, the areas and downwind distances were within a factor of two of those observed.

TABLE OF CONTENTS

KDFOC3

A NUCLEAR FALLOUT ASSESSMENT CAPABILITY

1. INTRODUCTION

The detonation of a nuclear device near the surface produces radioactive fission products that are swept up along with surface material. Significant amounts of radioactivity condense on available surfaces and fall back to the ground in a relatively short time. This fallout produces a potentially lethal hazard that must be evaluated for proper management of civil defense, evacuation, and war plans.

KDFOC3 is a computer program that has evolved over three decades for calculating and plotting gamma radiation fallout patterns from buried, surface and low-air detonations of nuclear explosives. Unlike some models, KDFOC3 methodology rigorously conserves radioactivity. Gamma dose rates or time-integrated doses at specified times after the detonation include the effects of a user-specified wind and the time-of-arrival of fallout.

This report includes the physical/mathematical model, the computational algorithms and user's manual, a FORTRAN listing, as well as an historical perspective of the code development.

Unless a nuclear fission device is fully contained upon denotation, it will inject radioactive particles into the atmosphere. Most of this debris is subsequently deposited on the earth's surface from minutes to years after an event. The potential hazard of this radioactive fallout was recognized by scientists even before the Trinity test at Alamogordo, New Mexico on July 16, 1945[1]. It is well known that peacetime testing of nuclear weapons in the atmosphere produced both local and global contamination. Worldwide concern existed between 1954 and 1963 before the limited test ban treaty was signed. Over the past several decades there has been continuing research and debate on the effects of nuclear fallout. Recently an entire issue of AMBIO[2] was devoted to the topic of the aftermath of nuclear

war. This rekindled international interest. The International Council of Scientific Unions[3] (SCOPE 28) chose KDFOC2 as the model upon which they based their conclusions.

1.1 Scope of Modeling Effort

Fallout is usually portrayed as consisting of two types: local and global. Local fallout reaches the surface in twenty-four hours. Global (intermediate and long-range) fallout is on particles that reach the surface at later times. Global fallout is generally associated with particles smaller than about 5 micrometers in radius. Most global fallout is deposited in latitudes of its origin by precipitation.[4] Its half-residence time in the atmosphere is weeks if it is initially injected into the troposphere and months to years if injected into the stratosphere. Because of radioactive decay, the global fallout γ-radiation hazard is reduced several orders of magnitude below that of local fallout.

Two processes which are not modeled by KDFOC3 that can deposit radioactivity on the surface from particles with negligible settling velocities are vertical diffusion and rainout. For surface and buried bursts at the high radiation levels considered here, vertical diffusion and rainout are considered second order effects; however, it is worthy to note that a low-yield surface burst could deposit significantly more radioactivity locally if detonated in a rain system.

The initial KDFOC was developed throughout the sixties. KDFOC2 development began in 1974 to address the problems of local fallout using more computer power than had previously been employed (see Appendix A). The primary objective of the KDFOC2 development task was to develop a local fallout model that:

- provided fast turn-around time on a computer;
- was continuous in all physical quantities as a function of yield, depth-of-burial, and height-of-burst;
- was sensitive to measurable winds;
- could address both radioactively dirty (fission) and clean (fusion) weapons;

- could accurately predict militarily significant radiation levels;

- could do tactical yield ranges; and

- compared reasonably well (i.e., within a factor of two) with Nevada Test Site (NTS) measured fallout patterns.

Over the years KDFOC3 has done all of these and has been employed in many fallout studies at Lawrence Livermore National Laboratory (LLNL)[5]; detailed documentation of the code, however remained elusive. Thus, the code has remained essentially an LLNL internal numerical tool. The purpose of this report is to provide a current document reflecting a general reprogramming and clean-up of the computer code which has made it an essentially "stand-alone" capability ready to be shared with other organizations. The resulting transportable code is termed KDFOC3.

1.2 Fallout Phenomenology

Detonation of a nuclear device of yield W [kt] in air or on the surface produces a fireball of approximately $30\ W^{1/3}$ meters in radius. If a device is detonated high enough in a fair weather atmosphere so the fireball does not touch the ground, then the local fallout is negligible. If a device is deeply buried, then the burst is totally contained and there is no injection of radioactivity into the atmosphere, thus, no fallout. Those detonations in-between produce local fallout modeled by KDFOC3.

During a nuclear detonation, everything in the device and its immediate surroundings vaporizes at extremely high temperature, forming a fireball. In all but deeply buried bursts, this fireball rushes upward, cooling by thermal radiation, expansion and entrainment of air and creating a strong, turbulent updraft. The center of the fireball is hottest, so it rises fastest, with the air viscosity quickly converting the rising bubble into a toroidal vortex. The vapors inside the nuclear fireball are intensely radioactive (See Fig. 1.2.1).

The residual radiation from nuclear explosions is of two distinct types: fission-product radionuclides which result from the radioactive decay of isotopes resulting directly from
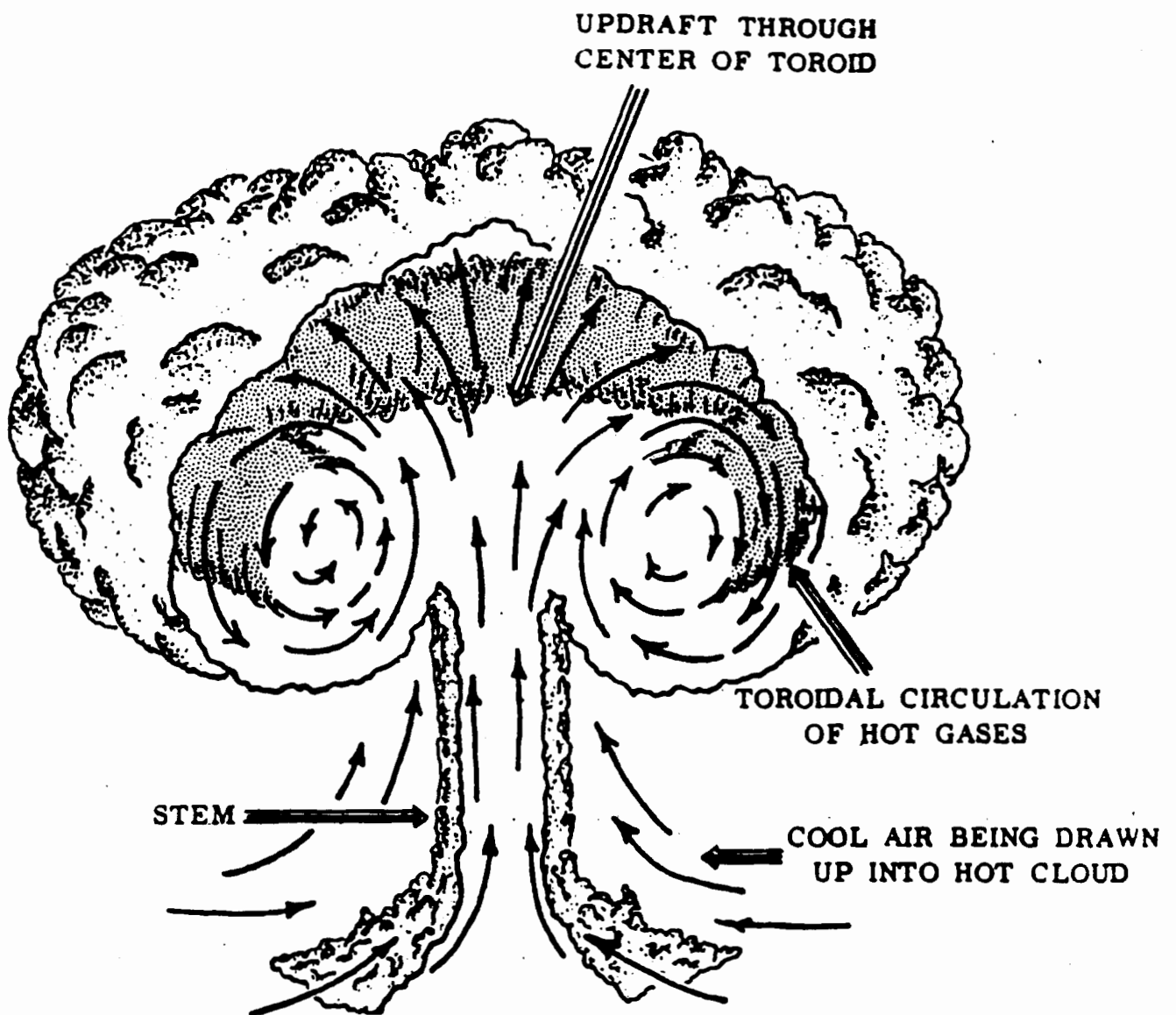
3

UPDRAFT THROUGH
CENTER OF TOROID

TOROIDAL CIRCULATION
OF HOT GASES

STEM

COOL AIR BEING DRAWN
UP INTO HOT CLOUD

Figure 1.2.1. Rising, Early-Time, Toroidal Radioactive Debris Cloud.[6]

4

a fission of ^{235}U, ^{238}U, or ^{239}Pu; and induced radionuclides due to neutron capture in material surrounding a nuclear explosion. In fission devices, because of the large amount of fission-produced radioactivity, induced radioactivity can usually be ignored; but in clean devices induced radioactivity at times can account for the major portion of the radiological hazard and, thus, must not be ignored.

As the fireball cools, the radioactivity condenses onto solid particles, including soil surfaces. The size of the fallout particles depends on the density of material in the rising debris cloud. A free-air burst, i.e., one whose fireball never touches the ground and which therefore involves nearly nothing condensable outside the device materials, produces tiny particles (a few tenths of a micrometer) too small to have sufficient gravitational settling to contribute to local fallout. When the fireball touches the ground, as in a surface burst, it tends to sweep up large quantities of pulverized soil from the crater and nearby surface areas. Small highly radioactive condensed particles agglomerate onto the dust, sand, and gravel that are swept up by the rising debris cloud. The most refractory nuclides condense onto particles first. Also, the largest and heaviest particles detrain first followed by smaller particles. This causes "fractionation." The refractories tend to be found on the largest fallout particles. For a given set of conditions, the smallest fallout particles with the most volatile nuclides rise highest and stay up the longest. Most smaller particles tend to be found in intermediate and long-term fallout, i.e., global fallout.

A buried nuclear detonation vaporizes the device as well as soil or rock that surrounds it. Soil and rock are melted creating a molten liner. More distant material is fractured. The buried burst, thus, has significantly larger particle sizes than the surface burst. Material at the surface above the detonation point is moved by spallation and by gas acceleration if the device is sufficiently deeply buried. The net result is that the overburden, the soil and rock above the device, is raised. This produces many fissures through which the radioactive gas percolates. This percolation deposits radioactivity on the overburden. The contaminated overburden is thrown upward, some of the heavier chunks on ballistic trajectories. Where

they hit the surface contributes to the ground zero circle area of radioactivity. When the lofted overburden returns to the surface, it also causes a radioactive "base-surge" cloud that moves radially outward. The overburden downward motion is called "bulk subsidence."

Meanwhile a buoyant rise at the center of the base-surge cloud continues accompanied by expansion of the hot gases created in the initial explosion. The termination of the buoyant rise forms a radially expanding main (or cap) cloud. It is smaller and lower than those formed for surface bursts. The size of the main cloud depends strongly on the scaled depth of burst and on the emplacement medium. Some deep bursts in hard dry rock form essentially no main cloud.

These events are illustrated in the sequence of photographs in Fig. 1.2.2 (taken from Ref. 7) for the Sedan event. Surface motion started just before 2 seconds after the detonation (Frame 1). The fireball broke through the surface just before 3 seconds (Frame 2). Frame 3 depicts the ballistic ejecta with the percolating hot gases. In Frames 4 and 5, several tens of seconds after the detonation, large chunks of material are seen still to be airborne and the base surge cloud is emerging into view. In the last frame at 6 minutes after detonation, the stabilized cloud with a large base surge is seen.

The final outward appearance of the radioactive stabilized cloud is of a broad base-surge cloud capped by a higher and narrower main cloud. Observations of these phenomena have prompted others to model buried burst airborne radioactivity as having two components, a base-surge cloud and a main cloud. Such models are competent at describing distant, relatively low level fallout data, but they do not predict the intense, close-in radioactive fallout immediately downwind of ground zero. It is clear that with the buoyant rise of the main cloud there is, at lower altitudes, a trailing, radioactive stem cloud just as in the case of a surface burst. This stem cloud is embedded within the base surge cloud. We find that prediction of the highest levels of close-in fallout from buried bursts is not possible without this embedded stem cloud; thus, it has been included in our modeling effort.
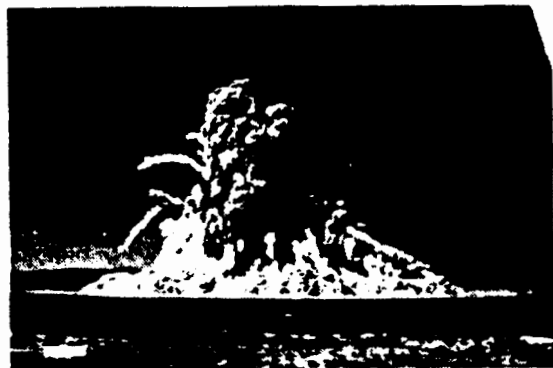
6

1 TIME = H + 1.9 sec.
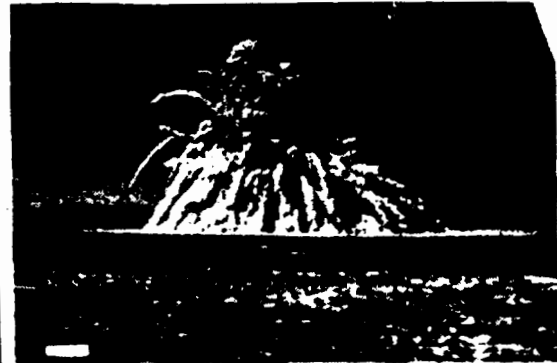
4. TIME = H + 27 sec.

2 TIME = H + 2.8 sec.

5 TIME = H + 39 sec

3 TIME = H + 4 0 sec

6. TIME = H + 6 min

Figure 1.2.2. Photographs of Sedan Event.[7]

2. THE KDFOC3 MODEL

KDFOC3 is an empirical model. The physical processes that are included have been motivated by extensive studies of film records and fallout data. The parameters of the model are based on measured NTS data. The empirical approach is necessitated by our goals of developing a fast running computer model. Further, a single computer code to calculate the full suite of nuclear explosion, gas-soil hydrodynamics, particle-wind interaction, is beyond the capabilities of present computers—and available data.

2.1 Dose-Area Integral

There are three types of ionizing radiation associated with residual radioactivity, alphas, betas, and gammas. Alphas, which are helium nuclei, are emitted spontaneously with high energy from unburned fissile material. Betas, which are high energy electrons, result from the radioactive decay of the fission-products and neutron-induced radionuclides. These are emitted by daughter radionuclides as they deexcite following β decay. Gamma radiation consists of high energy photons. The charged alphas and betas have sufficiently short ranges in air and tissue to be of little concern to individuals with even minimal sheltering. If not inhaled or ingested, their primary hazard is to the skin, and then only if the radioactivity comes in contact with it. The uncharged gamma radiation, however, has sufficient penetrating power to be an external hazard to the whole body. At early times any radiological procedure that adequately deals with gamma radiation should also effectively deal with alpha and beta radiation. Gammas are the dominating hazard shortly after nuclear detonation, when they can easily cause death. However, because of rapid decay of gross fission products, the possibility of death from gammas rapidly diminishes; over the long-term, other radiological pathways become more important considerations.

Fission Yield

The refractories tend to be on the larger fallout particles and the volatiles on the smaller particles. As an approximation to keep KDFOC3 a fast computer code, its formulation

integrates over different levels of volatility and deals only with gross-fission products, not individual nuclides. This is accomplished by using a gross fission product decay law to calculate doses rather than individual nuclide decays and dose conversion factors. The empirical location-dependent gamma decay curves measured at NTS range from $t^{-2.0}$ to $t^{-0.9}$ for fission weapons, depending on time and location in the radiation field. For adjusted gross-fission products, Glasstone and Dolan[6] give the $t^{-1.2}$ decay law (see Fig. 2.1.1). This is the curve that we use to determine time-integrated dose.

The calculated radiological dose rate in roentgens, three feet above a smooth plane one hour after detonation with 1 kt per square mile of gross fission products uniformly deposited provides us with a conversion factor between deposited 1-kt of fission products and dose rate.

$$K = 3000 \frac{\text{R}}{\text{hr}} * \frac{\text{mi}^2}{\text{kt}} \qquad (2.1.1)$$

$$W_{FPY} = K * \text{yield (kt)}$$

Fusion Yield

For clean devices, the induced radionuclides from neutron capture have decay curves different than fission-products. To incorporate induced radioactivity into gross-fission products requires definition of a fission equivalent yield (FEY). For penetrating radiation, the biological hazard is directly proportional to the energy released. For acute, militarily significant radiation, the primary time frame of interest is about ten minutes to fifty hours. During this time, the gross-fission products release approximately 2.0×10^{23} MeV of gamma energy from a 1 kt weapon. Using energy released by radionuclides induced from fusion neutrons during the 10 minutes to 50 hour time period, we define the fission-equivalent yield as[8]

$$W_{\text{IR}} = \frac{\text{kT}}{2 \times 10^{23}} \sum_i \int_{10m}^{50h} \frac{a_i \epsilon_i e^{-t/\tau_i}}{\tau_i} dt \qquad (2.1.2)$$
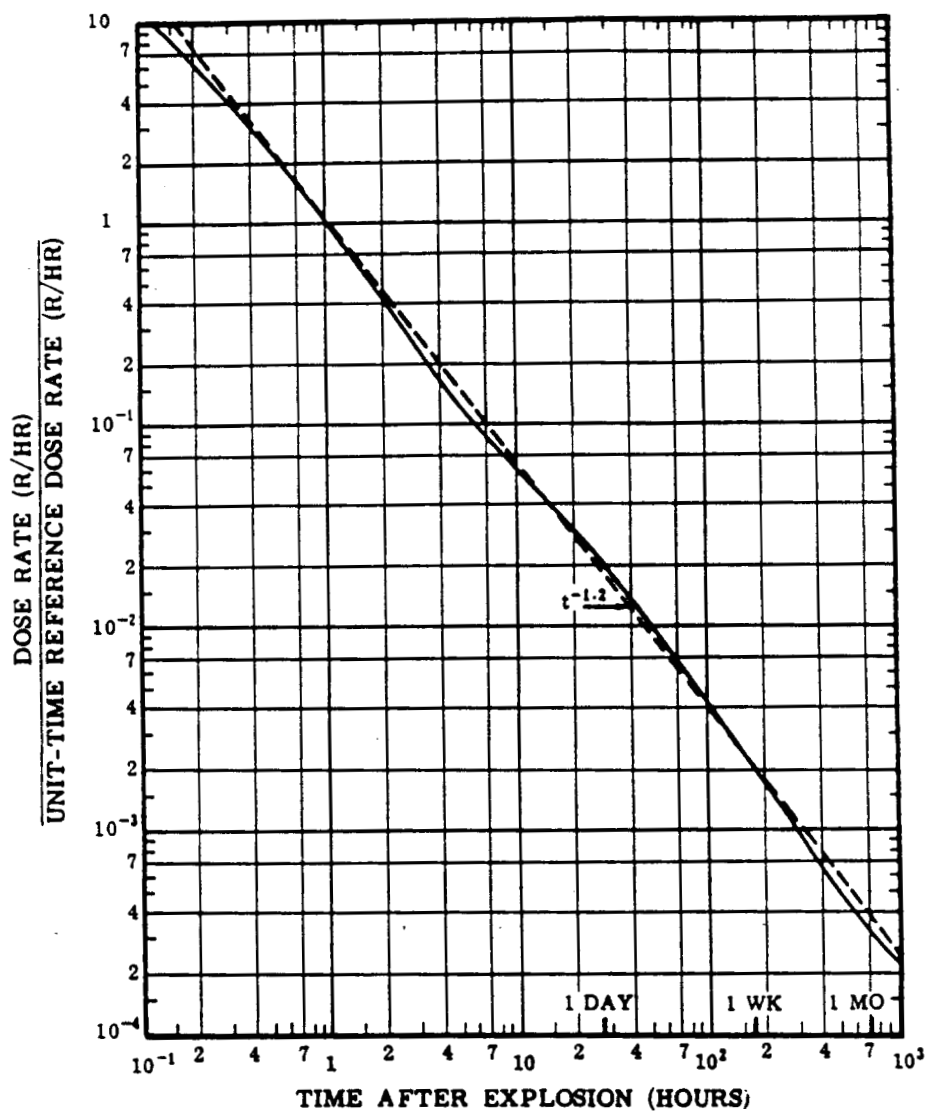
where

Figure 2.1.1. Adjusted Gross-Fission Products Decay Curve and the $t^{-1.2}$ Decay Law.

i is the index of a particular radionuclide;

a_i is the number of radionuclide i at 10 minutes;

ϵ_i is the gamma decay energy, MeV; and,

τ_i is the mean life for decay.

Calculations of induced radioactivity for a standard soil,[9] chosen as Chester Dry Soil[10] for various weapon configurations have been made. Variations in induced radioactivity were found for differing soils and devices. For thermonuclear weapons with substantial fusion, which have not been designed to suppress neutrons, a rule-of-thumb has emerged: for internal activation, KDFOC3 incorporates 20 tons per kiloton of fusion; for soil activation for surface bursts, 80 tons per kiloton of fusion, and for buried bursts an additional 80 tons per kiloton of fusion yield.[10] For example, a hypothetical buried, weapon would produce a W_{IR} equal to $\sim$ 0.18 kt of gross-fission products per kt (of fusion) if no effort had been made to suppress its neutrons. If smeared uniformly over one square mile, it would result in a radiological hazard of about 1000 rems from ten minutes to 50 hours. Thus, our induced radioactivity rule-of thumb is for a well-defined device, for a standard soil, and is meant to be representative of induced radioactivity expected from fusion yield. For actual designs, the induced activity can be provided by the code user by overriding the neutron-activation module (see Section 3.3).

Total Fission Equivalent Yield

The fission equivalent yield [kt] is given by the expression

$$W_{FEY} = W_{FPY} + W_{IR} \ .$$

(2.1.3)

where W_{FPY} is the fission product yield and W_{IR} is the induced radioactivity.

11

Ground Zero Circle

The ejecta and prompt neutron capture contamination about ground zero are empirically modeled in KDFOC3 by the "ground-zero circle" routine. Let R_{GZ} be the radius of the ground-zero circle given by

$$R_{GZ} = \max\left\{1346\ W^{0.31}, R_{\text{MC}}, R_{\text{BS}}\right\} \quad [\text{m}] \tag{2.1.4}$$

where R_{MC} is the main cloud stabilized radius and R_{BS} is that for the base-surge cloud. Empirically, we find the activity drops nearly exponentially. If $\dot{D}(0)$ is the dose rate at ground zero at H + 1 hrs, we write for radius r

$$\dot{D}(r) = \dot{D}(0)\ e^{-kr/R_{Gz}} \quad [\text{rem/hr}] \tag{2.1.5}$$

where k is a factor depending on the scaled depth of burial. The ground-zero-circle dose accounts for the ballistic trajectories of the very large particles. It is added to the dose calculated from fallout sized particles.

2.2 Air-Borne Activity

Not all of the created radioactivity is accounted for in local fallout patterns. Data show that about 75% from FEY of a surface burst is on local fallout-sized particles with radii greater than 5μm. The other twenty-five percent or so, is found either buried in the crater region or on particles sufficiently small that they have negligible settling velocity.

Vent Fraction

If DOB is the depth of burial [ft], then the scaled-depth-of-burial (SDOB) is defined as

$$\text{SDOB} \equiv \text{DOB}/\text{W}^{0.294} \tag{2.1.6}$$

for total yield, W [kt]. If SDOB is larger than about 200 ft, the activity is usually contained.

12

To account for explosions for SDOB < 200 ft, the vent fraction, FV, is defined. KDFOC3 uses an FV based on measured data roughly shown in Fig. 2.2.1. For a surface burst, FV ~ 0.75.

The effective fallout yield at H + 1 hour (intensity-area integral) then becomes

$$FV * W_{FEY} \ . \tag{2.1.7}$$

in units of kilotons. It is the conservation of this quantity in the fallout pattern that leads to conservation of radioactivity and makes KDFOC3 more credible at low radiation levels than some other models. Many numerical fallout codes, including the original KDFOC, SEER II, SEER III and LASEER[11] do not conserve this quantity. It is only because most cases of interest are close-in fallout that these other codes do not at times obtain much more radioactivity on the ground than was created by the device.

Measurements of the actual intensity-area integral indicate about three-quarters of the fission products produced are on particles greater than 5μm radius. The fraction of activity on particles greater than 25μm radius is about sixty percent. The shielding provided by natural terrain is about 30%. Thus, for calculating dose from fission products, the effective 1-kt per square mile hazard reduces to ~950 R/hr at H + 1 hour. This is nearly the same value used in DELFIC, where the fraction of activity on particles greater than r = 25μm is very close to the value used in KDFOC3. This is an interesting coincidence since the two codes were developed independently.

2.3   The Effective Cloud Model

The empirical establishment of KDFOC3 initial conditions may be conceptualized as a time-reversal process (Fig. 2.3.1) in which the fallout particles are projected from their landing points backward in time to an effective initial fallout cloud at 5 minutes after the detonation. This "effective" cloud for a ground burst is chosen with an initially tapered stem cloud and main cloud located over ground zero (see Fig. 2.3.2). To avoid the very complex problem of accurately modeling cloud rise, we empirically choose a few parameters

13
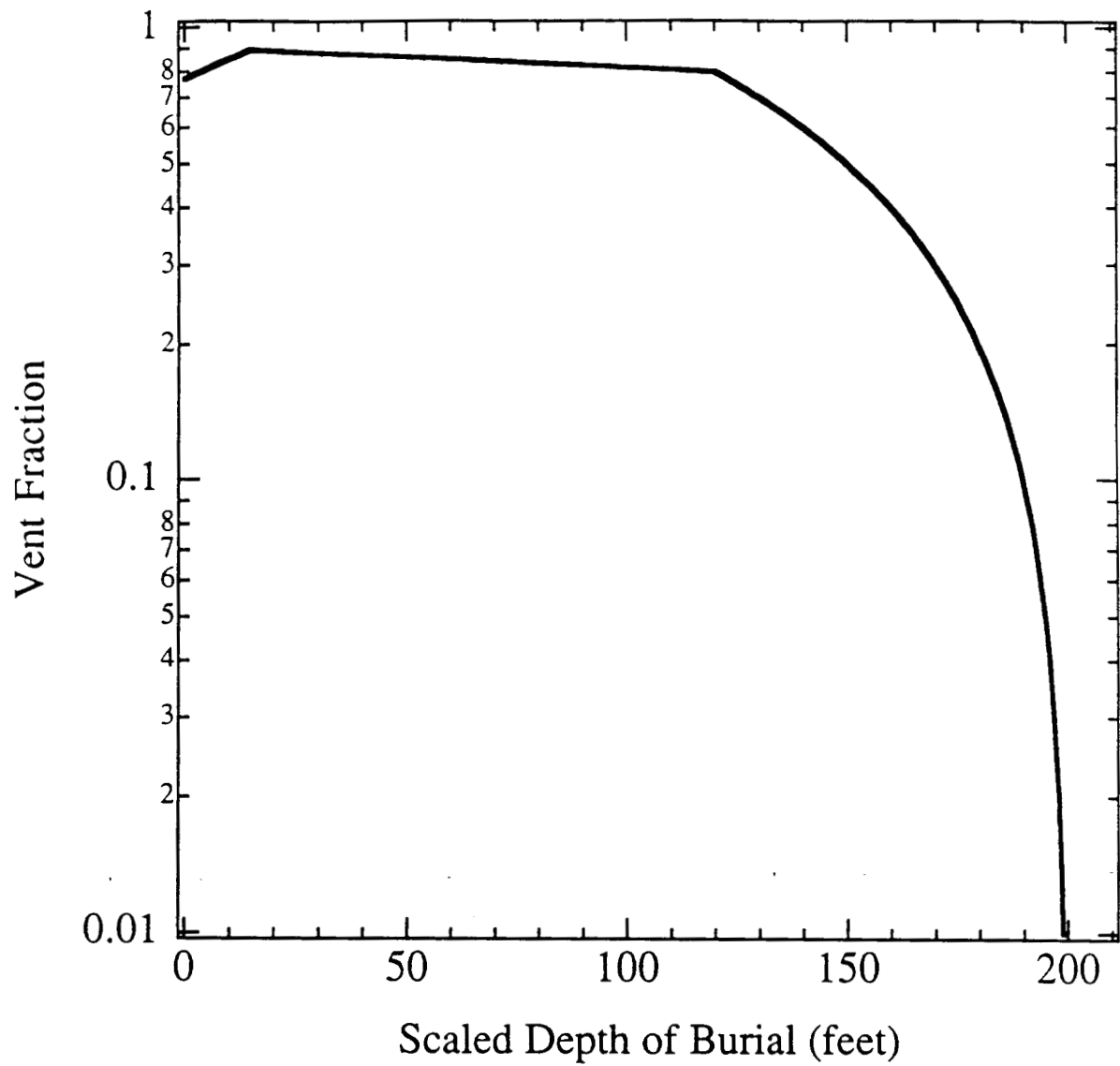
Figure 2.2.1. Vent Fraction Curve (fv) for Surface and Buried-Bursts.
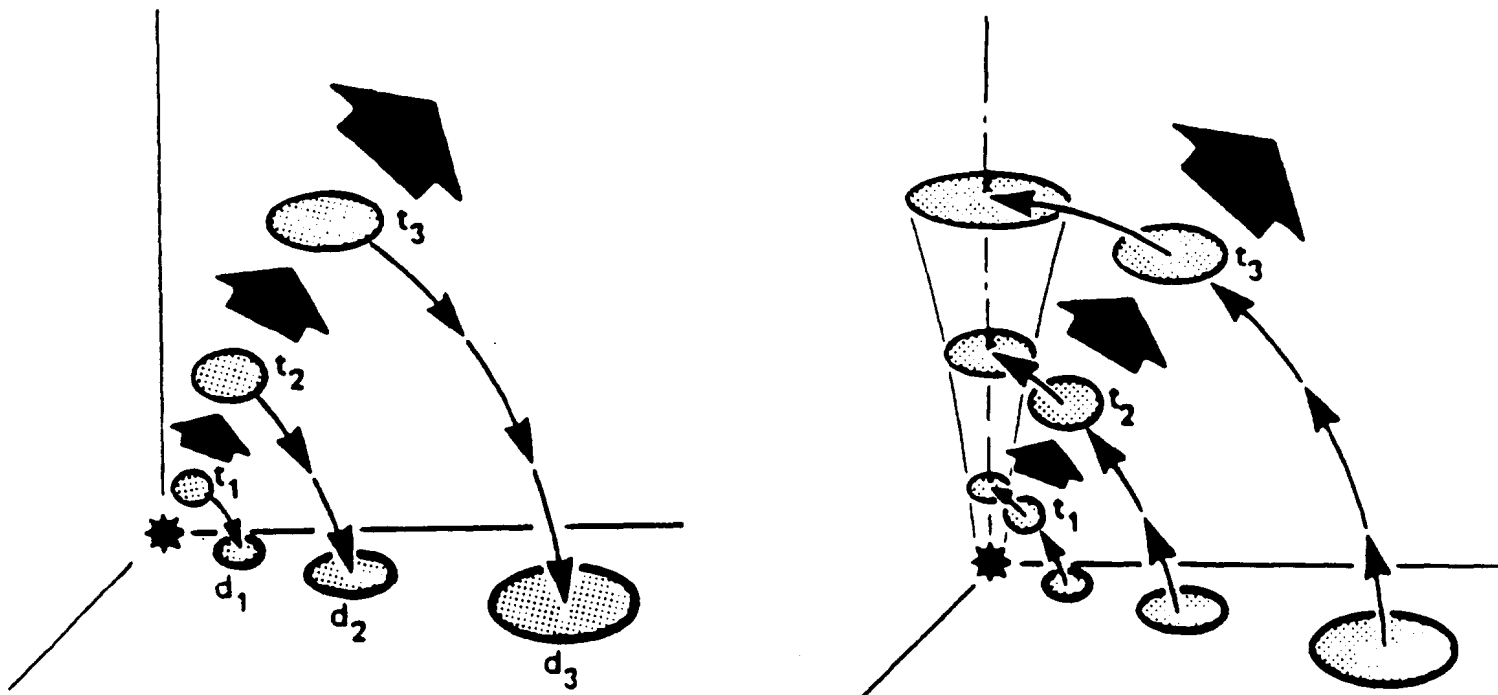
**Figure 2.3.1.** Schematic of Time-Reversed Disc-Tosser Model.

to assign an appropriate distribution of debris with respect to altitude and particle size. The success of our procedure is tested by the model's ability to fit all the relevant NTS data. We hoped to achieve an agreement within a factor of several for both clean and dirty devices. We actually obtained agreement with a standard deviation of about 40% (See Fig. 2.3.3).

The essence of the effective-cloud approach is to initially distribute radioactivity in a manner that accounts for variation with altitude, with "cloud radius," and particle size. KDFOC3 has a maximum of three radioactive debris clouds (see Fig. 2.3.2). It always has a main and stem cloud. The initial stem and main cloud distributions describe the cloud-rise and stabilization episodes. The tops, bottoms, and radii of the main cloud as a function of yield for surface bursts are given in Figs. 2.3.4 and 2.3.5. There are large deviations about mean values for these quantities. A minimum standard deviation of at least 25% is apparent in the data. For cloud tops and thicknesses this would seem partially due to different atmospheric stability conditions. Fluctuations like these have been modeled by hydrodynamic calculations which include the effects of relative humidity of atmospheric soundings. These models, however, do not account for much of the variability. Thus, we have not felt compelled to include the atmospheric stability factor in KDFOC3. Its effect on local fallout patterns is not crucial.

Fallout deposition data for buried nuclear explosives require inclusion of a radiologically hot, wind-driven stem cloud, embedded within the base-surge cloud. This cloud has proven necessary to model the hot radioactive gas as it percolates up through the crushed overburden, causing radioactive ejecta and fallback. The dimensions of this tapered cloud are related to main cloud dimensions by:

$$R_{sc,top} = R_{mc}/3 \qquad \text{the radius at the top of the stem,}$$
$$R_{sc,bot} = 3 * R_{FB}, \qquad \text{the radius at the bottom of the stem,} \qquad (2.3.1)$$
$$H_{sc,top} = H_{mc,bot} \qquad \text{the altitude of the top of the stem,}$$
$$H_{sc,bot} = H_{gz} \qquad \text{the altitude of the bottom of the stem}$$

SURFACE BURST
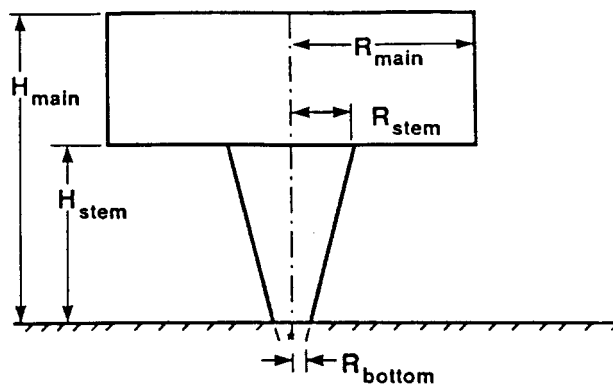
SHALLOW BURST
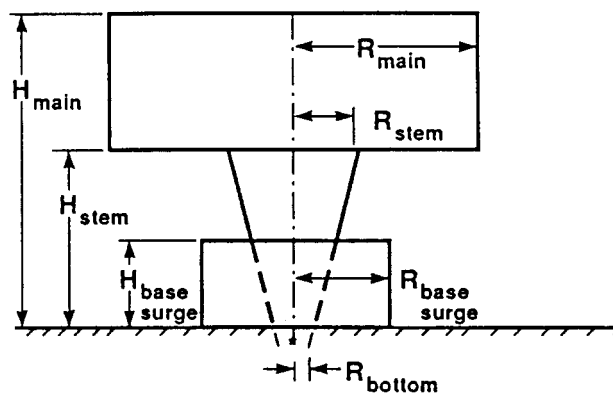
DEEP BURST
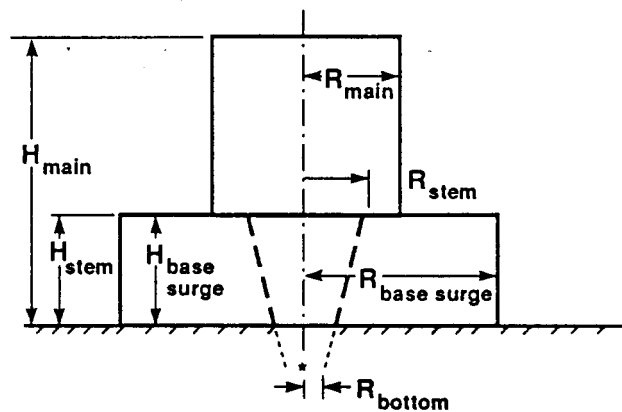
Figure 2.3.2. Schematic of KDFOC3 "Visible Cloud Configurations" at Stabilization.
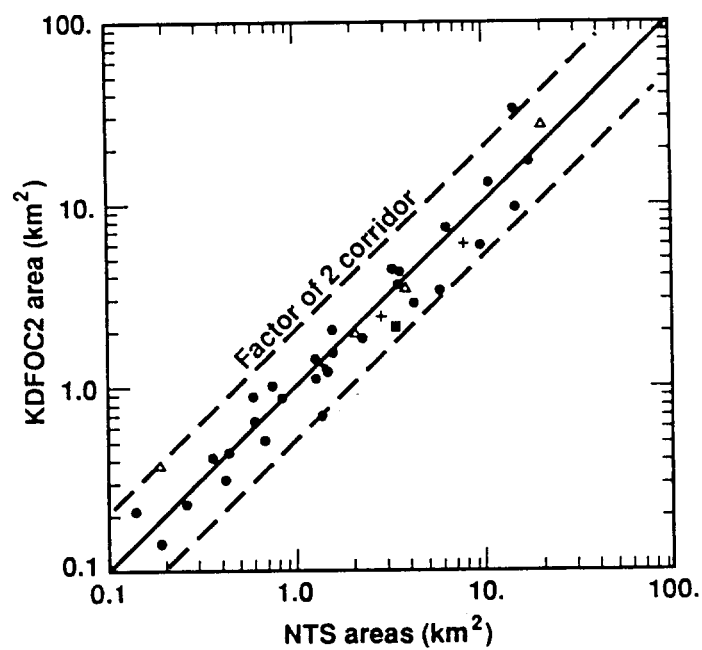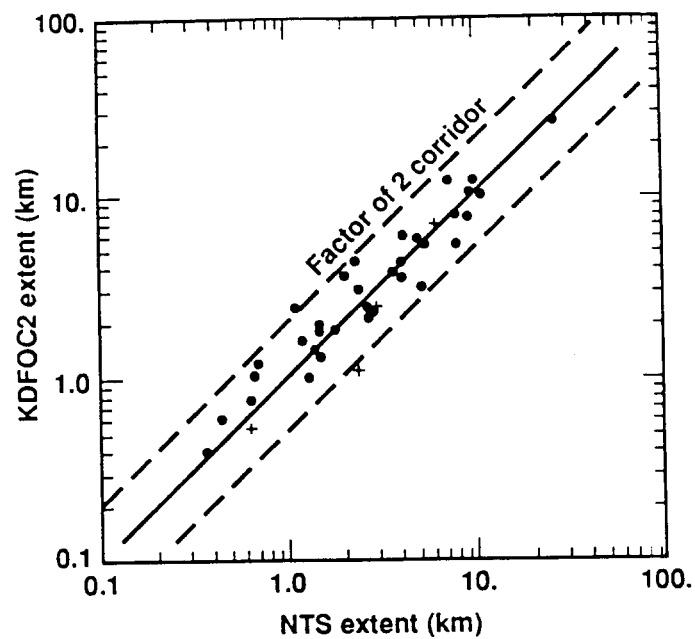
Figure 2.3.3. Comparison of NTS Data and KDFOC3 Downwind Extents and Areas, where + is Little Feller II areas/extent multiplied by 100 and △ is Schooner areas divided by 10.

CLOUD TOPS (M)

E-05

3
2
E+04

3
2
E+03

3
2
E+02

3
2
E+01

3
2
E+00

MAIN

STEM

E-03   2 3   E-02   2 3   E-01   2 3   E+00   2 3   E+01   2 3   E+02   2 3   E+03   2 3   E+04

W, TOTAL YIELD IN KT

Figure 2.3.4. KDFOC3 Cloud Tops and Bottoms Versus Yield for Surface Bursts.
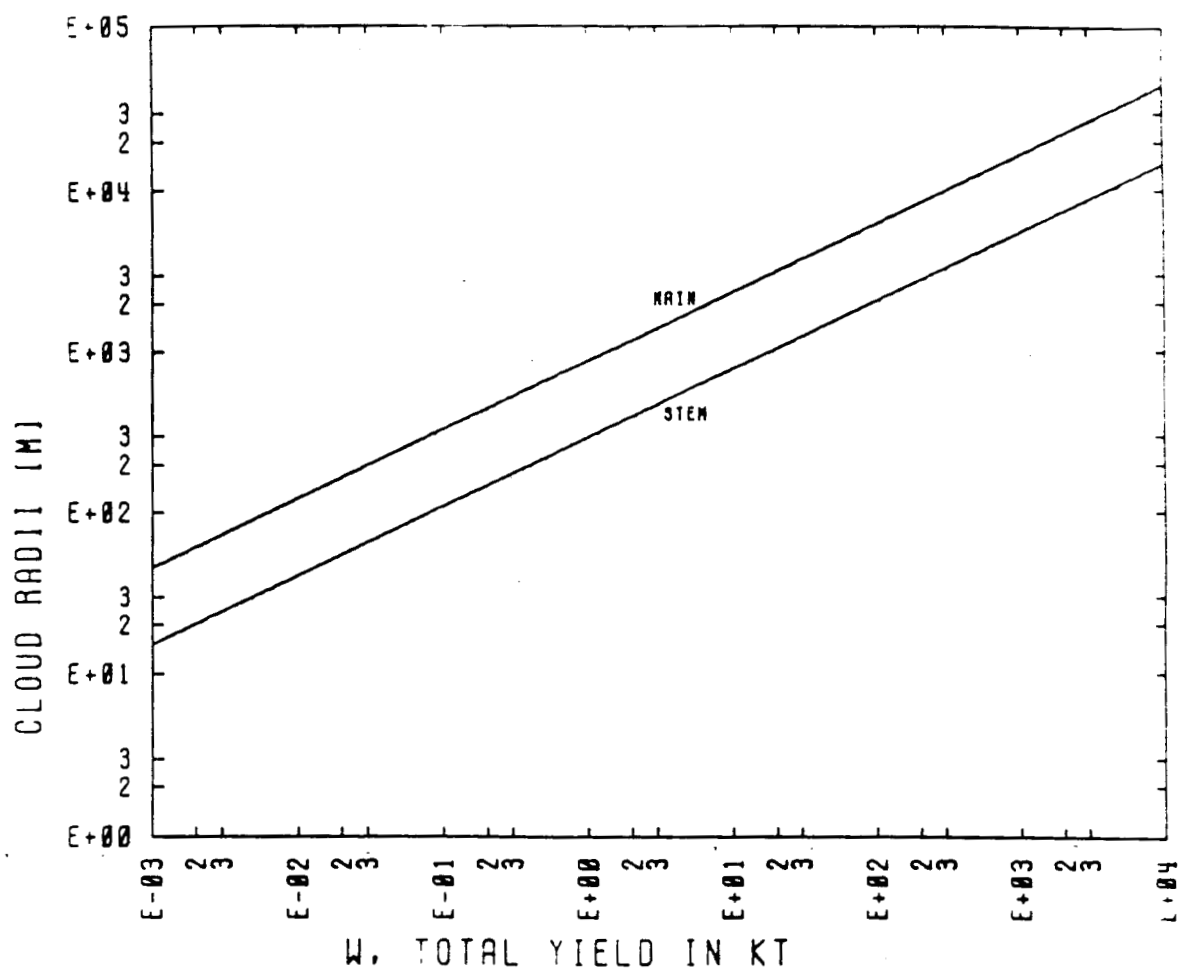
Figure 2.3.5. KDFOC3 Main Cloud Radius at Five Minutes for Surface Burst.

The slope of the stem cloud follows

$$dR/dz = \frac{R_{sc,top} - R_{sc,bot}}{H_{sc,top} - H_{sc,bot}} ,$$

where: R_{mc} is the radius of the main cloud,

$H_{mc,bot}$ is the altitude of the bottom of the main cloud,

$R_{FB} = 30 \ W^{1/3} \ [m]$ is the fireball radius,

H_{gz} is ground zero altitude.

To reproduce the highest intensity fallout patterns, the bottom of the stem was found to require a radius of approximately three times the initial fireball radius.

The curves in Figs. 2.3.6 and 2.3.7 show the KDFOC3 values of the main cloud tops and radii for buried explosives. The top and radius of the base-surge cloud are shown in Figs. 2.3.8 and 2.3.9. The bottom of the main cloud is chosen as the top of the base-surge cloud for deep-burial, i.e., for scaled-depth-of-burial, (SDOB $\geq 10 \ W^{.294}$ [m]). For shallow burial, linear interpolation to determine the bottom of the main cloud with respect to SDOB is made between values in Figs. 2.3.4 and 2.3.8.

Activity-Size Distribution (ASD)

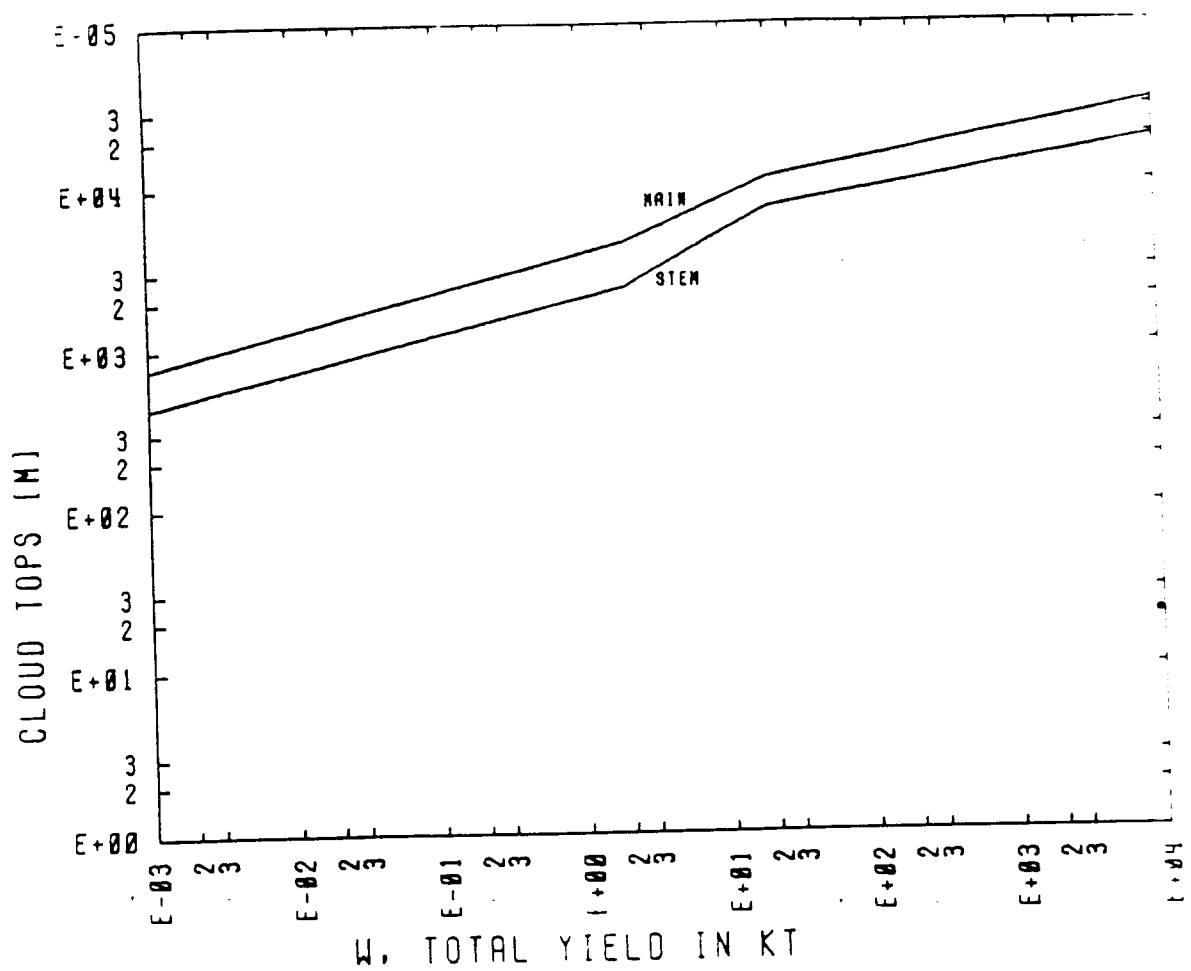Data indicate that a bifurcation of particle sizes occurs in the condensation processes of a nuclear debris cloud. Thus, we consider both "small" and "large" size particle distributions. We assume a fraction, u_L, of the radioactivity is placed on the large size distribution and the remainder, $u_S = 1 - u_L$, is placed on the small size distribution. The ASD is represented by a bimodal, lognormal distribution in particle radius, r. That is, for $5 \leq r \leq 500 \ \mu$m, with $k=1$ for "small," $k=2$ for "large",

$$ASD(r) = n \sum_{k=1}^{k=2} u_k B_k(r, \bar{r}_k, \delta_k) \quad \text{where} \tag{2.3.2}$$

$$B_k(r, \bar{r}_k, \delta_k), = \frac{1}{\delta_k r (2\pi)^{1/2}} \exp[-1/2\{ln(r/\bar{r}_k)/\delta_k\}^2] \quad \text{and} \tag{2.3.3}$$

$\bar{r}_k$ is the median (geometric mean) particle radius, δ_k is the geometric standard deviation and n is an overall normalization factor.
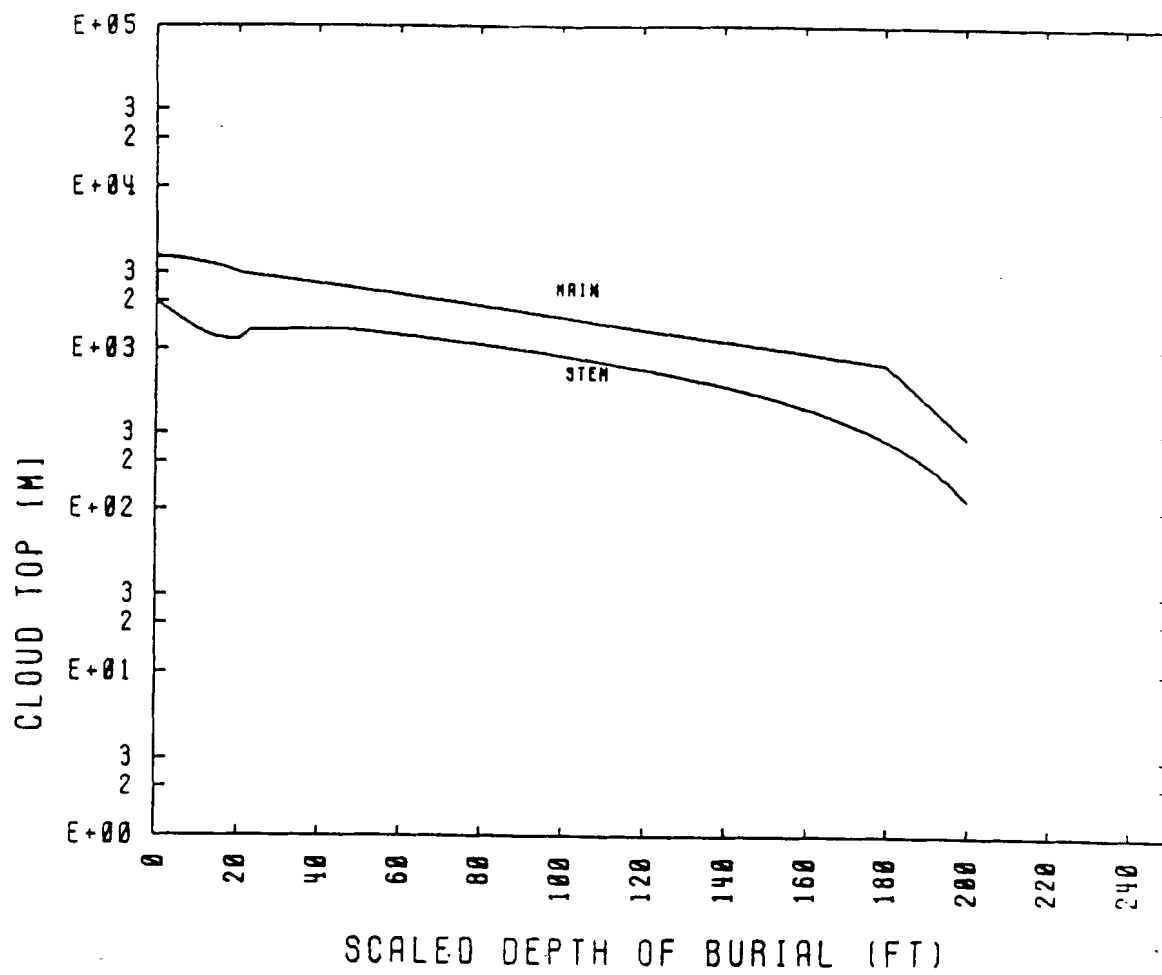
Figure 2.3.6. KDFOC3 Main Cloud Top for Buried Burst.

22
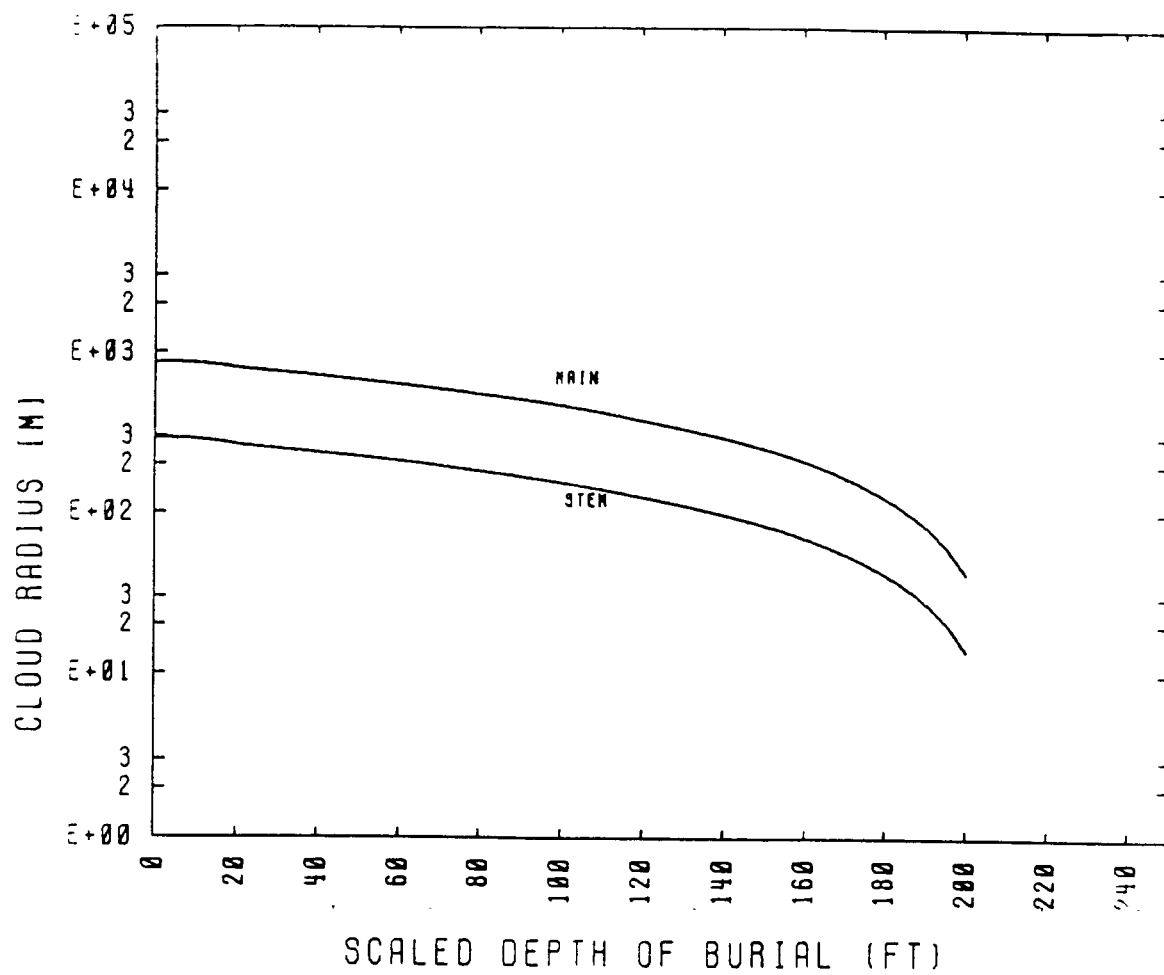
Figure 2.3.7. KDFOC3 Main Cloud Radius for Buried Burst.

23
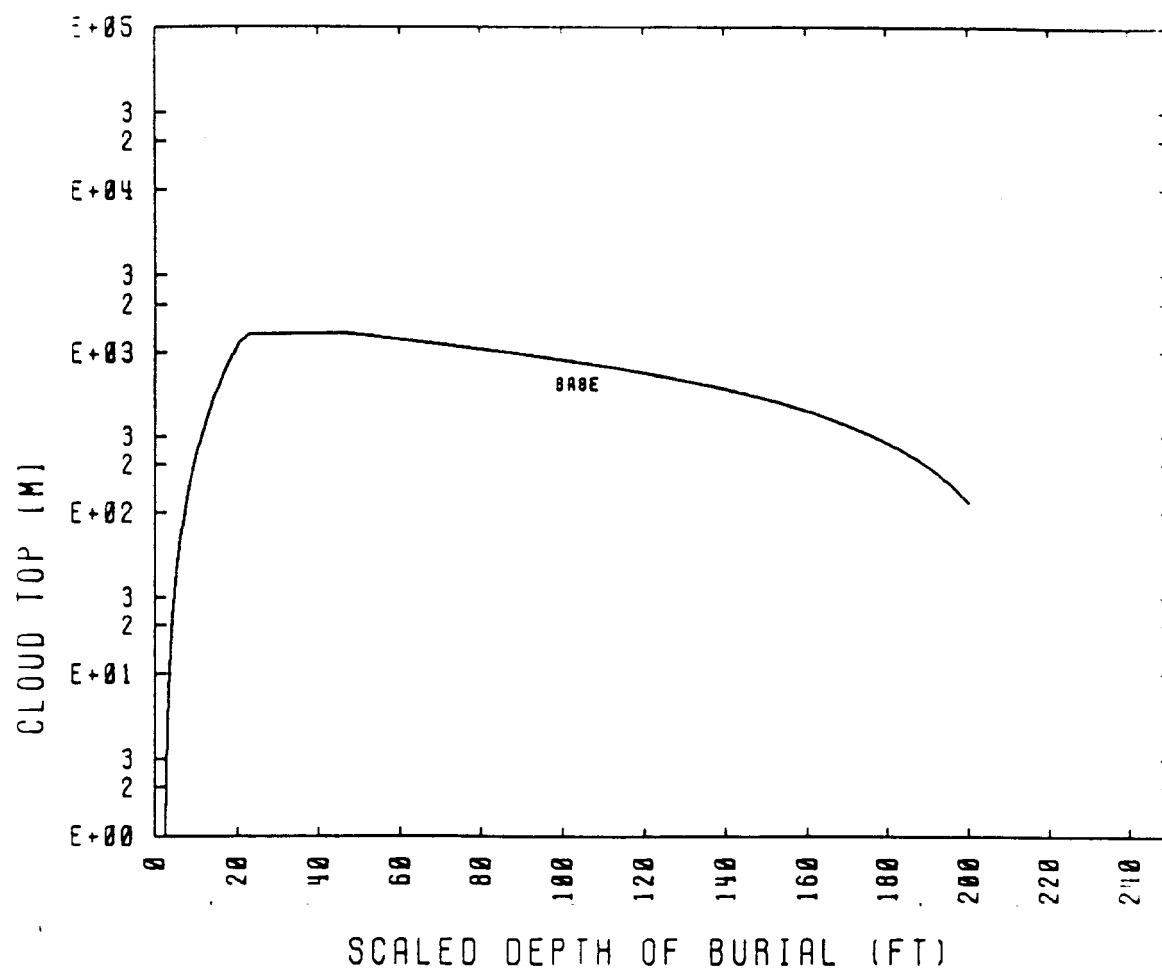
Figure 2.3.8. KDFOC3 Base-Surge Top.
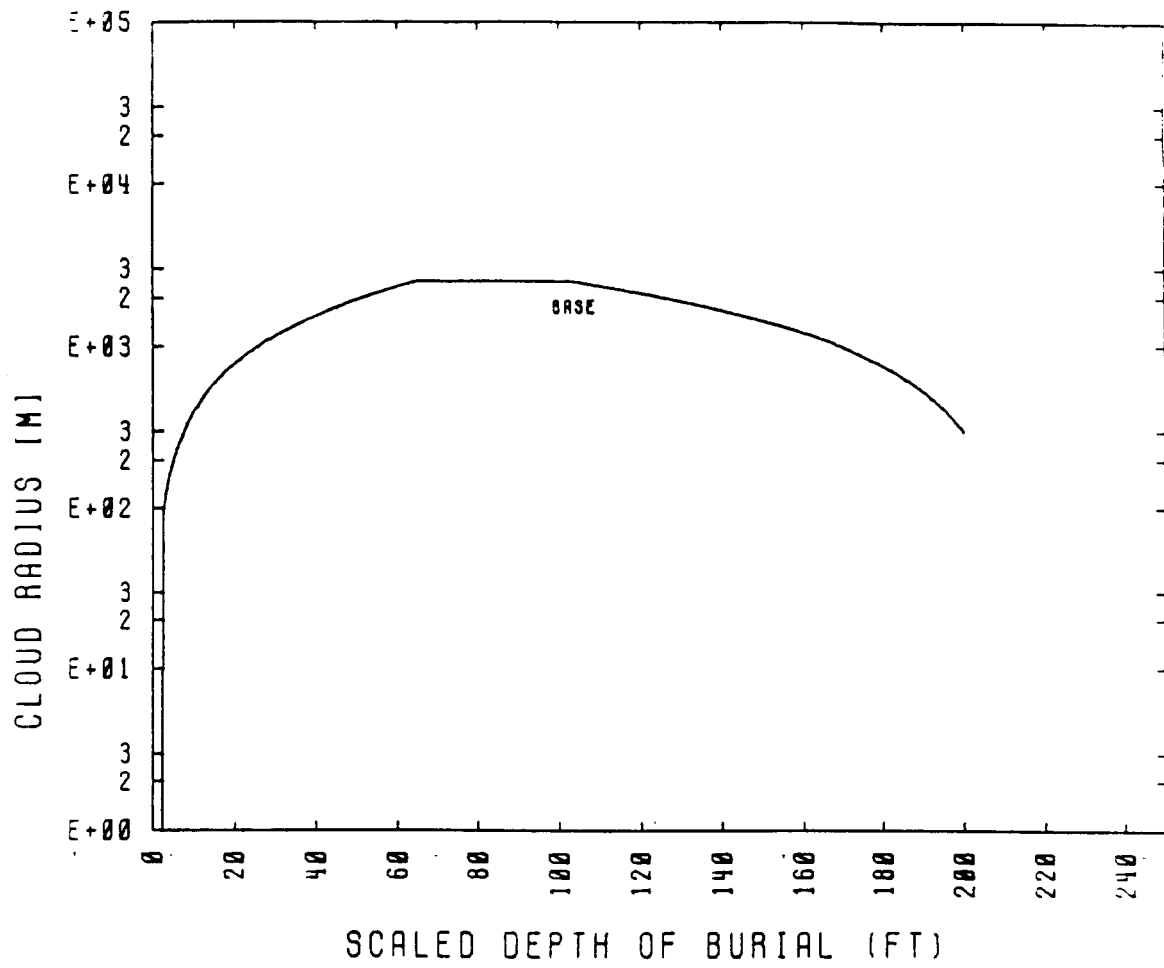
Figure 2.3.9. Base-Surge Radius.

The appropriate choice of the normalization factor, n, gives

$$1.0 = \int_{5 \ \mu m}^{500 \ \mu m} ASD(r)dr \ .$$

(2.3.4)

To obtain an estimate of the activity-size distributions, $B_k(r)$, the "visible" activity-size distribution obtained for the surface-burst SMALL BOY event shown in Fig. 2.3.10 was examined. The hydrodynamic activity-size distribution, which relates the radioactivity to a settling velocity, is not exactly the same as the visible activity-size distribution; however, it is expected that the visible size distribution is a good starting point for determining the hydrodynamic size distribution. Even if there are substantial hydrodynamic differences between fallout particles and 2.5 gm/cm^3 spheres, as long as our range of settling speeds is large enough and the choice of the $ASD(r)$ is general enough, an appropriate settling speed for each element of activity (disc) should result from empirically determining the parameters specifying our effective cloud.

A five-parameter, non-linear, multiple regression analysis of the SMALL BOY ASD data with the bimodal, lognormal distribution function resulted in the following parameters for a surface burst (see Fig. 2.3.10):

$$u_L = 0.23$$

$$\bar{r}_s \approx 14.44 \quad (\ln \bar{r}_s = 2.67)$$

$$\delta_s = 4.01 \quad (\ln \delta_s = 1.39)$$

(2.3.5)

$$\bar{r}_L \approx 151.41 \quad (\ln \bar{r}_L = 5.02)$$

$$\delta_L \approx 2.69 \quad (\ln \delta_L = 0.989)$$

For deep buried bursts (scaled depth of burial more than 15 meters), the ASD parameters were determined for KDFOC by Knox et al.,[12] and were partially based on SCHOONER data (See Figure 2.3.11). The bimodal, lognormal parameters that they
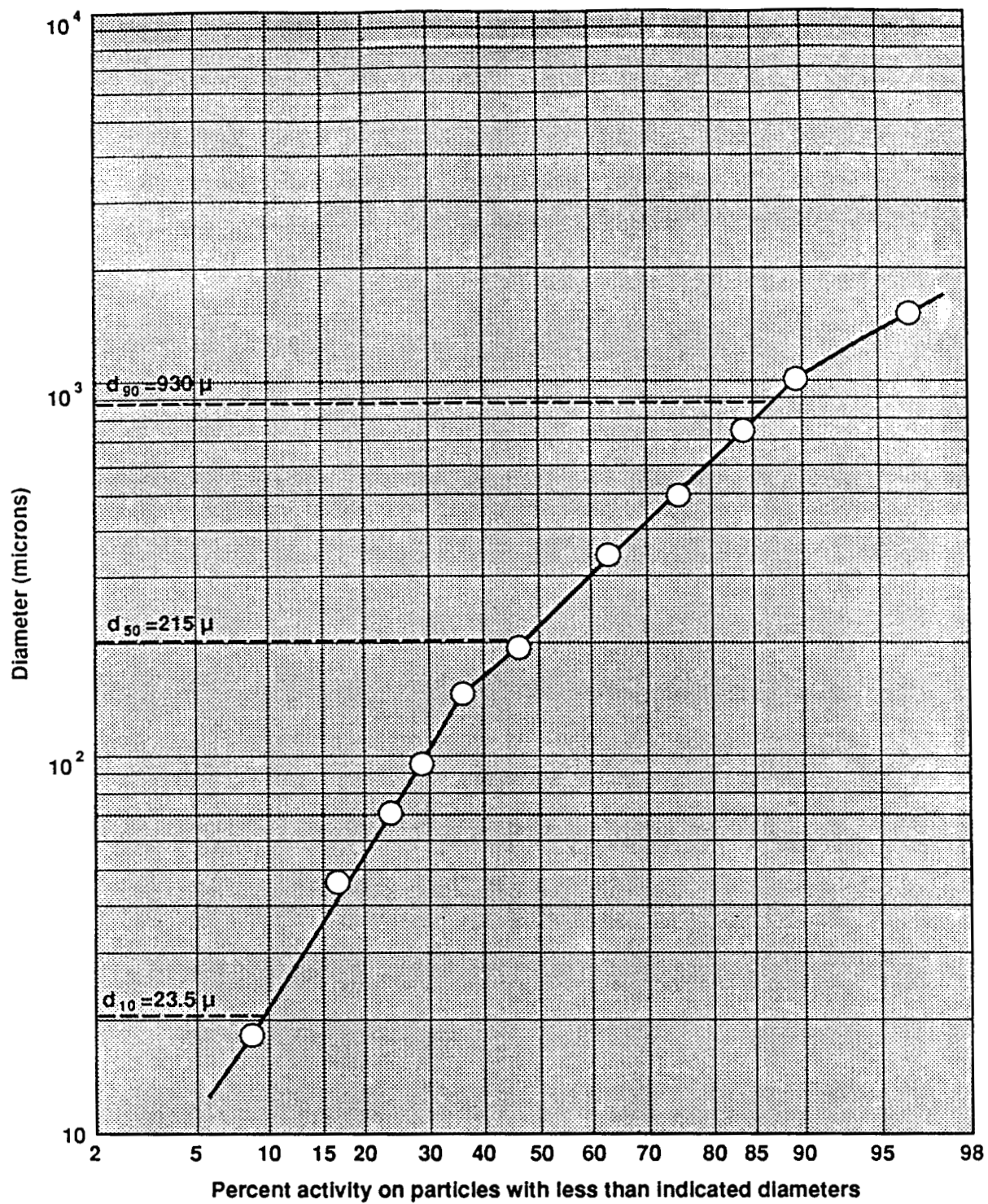
Figure 2.3.10. SMALL BOY activity-size distribution and fit given by Equation 2.3.5.

found were:

$$u_L \approx 0.65$$

$$\bar{r}_s \approx 90.02 \quad (\ln \bar{r}_s = 3.8)$$

$$\delta_s \approx 2.01 \quad (\ln \delta_s = 0.7) \tag{2.3.6}$$

$$\bar{r}_L \approx 298.87 \quad (\ln \bar{r}_L = 5.7)$$

$$\delta_L \approx 1.82 \quad (\ln \delta_L = 0.6)$$

The median size is about twice the size for the surface burst.

The ASD for shallow burial is a linear interpolation on the SDOB between the surface ASD and the deep burial ASD. In comparing the altitude and size distribution for buried bursts with surface bursts, the stem and main clouds for buried bursts have a much larger fraction of the radioactivity on larger particles which are lower in the cloud than for surface bursts. u_L ranges from fifty to eighty percent in contrast to twenty percent in the surface burst case. The base-surge cloud appears to have about eighty percent of its activity on B_1 (See Fig. 2.3.12). This is expected, as the base-surge visually appears to be a resuspension effect. The smaller radioactive particles are more apt to be resuspended and diffused by base-surge turbulence than larger particles.

Activity-Height Distribution (AHD)

The key to empirically simulating cloud rise is to find the appropriate activity on each of NxMxJ discs, which are indices referring to cloud, height and particle-size, respectively. Besides the Activity-Size Distribution, KDFOC3 uses the activity-height distribution (AHD). The ASD and AHD are highly correlated in affecting fallout patterns. This is partially accounted for by using the parameter, u_L. Also, the empirical derivation of parameters depends on choosing spherical particles of density 2.5 g/cm³. A different choice would result in different AHD parameters.
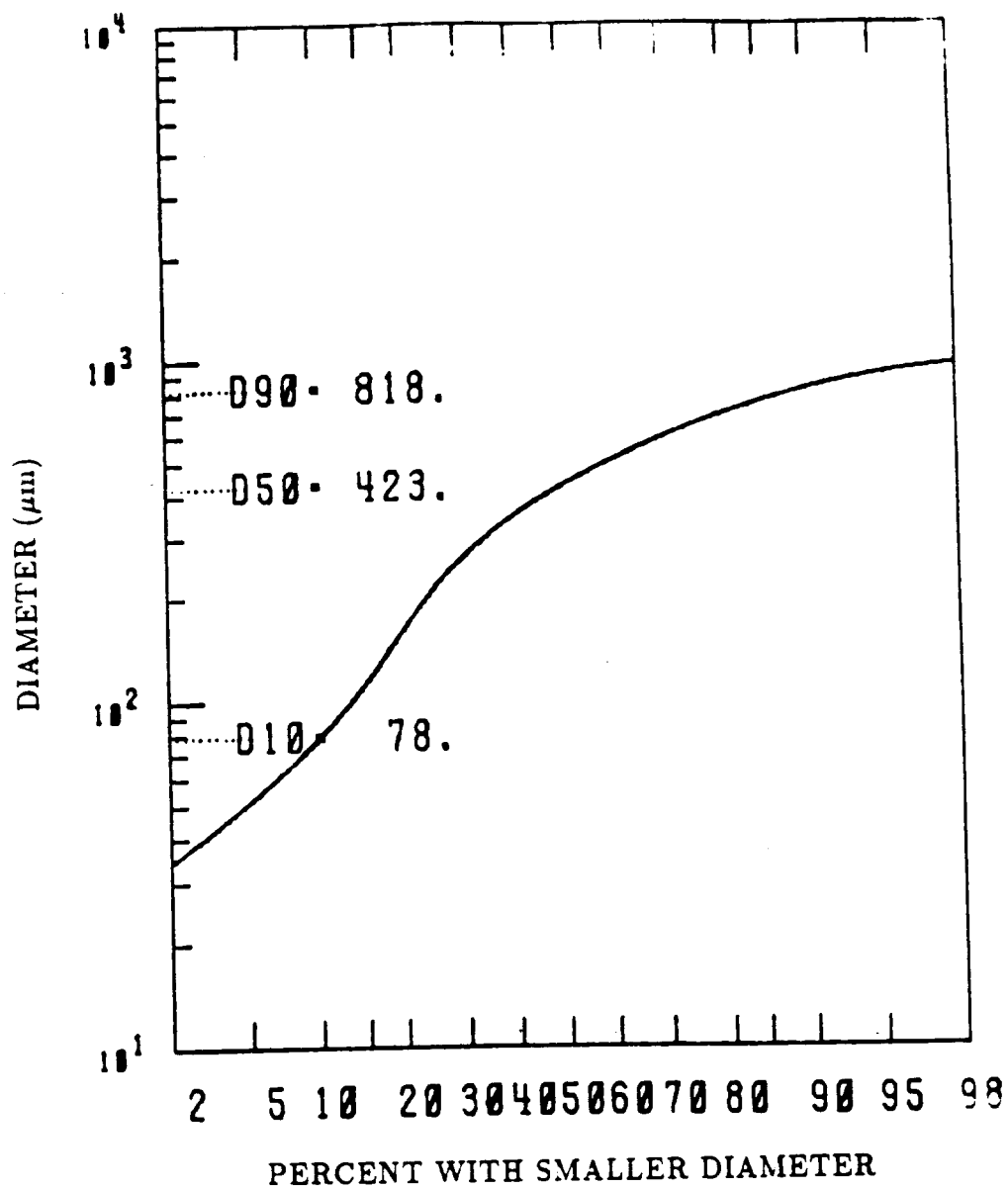
Figure 2.3.11. KDFOC3 Buried-Burst Activity-Size Distribution. D90, D50, and D10 are the 90th, 50th, and 10th percentile diameter in micrometers, respectively.
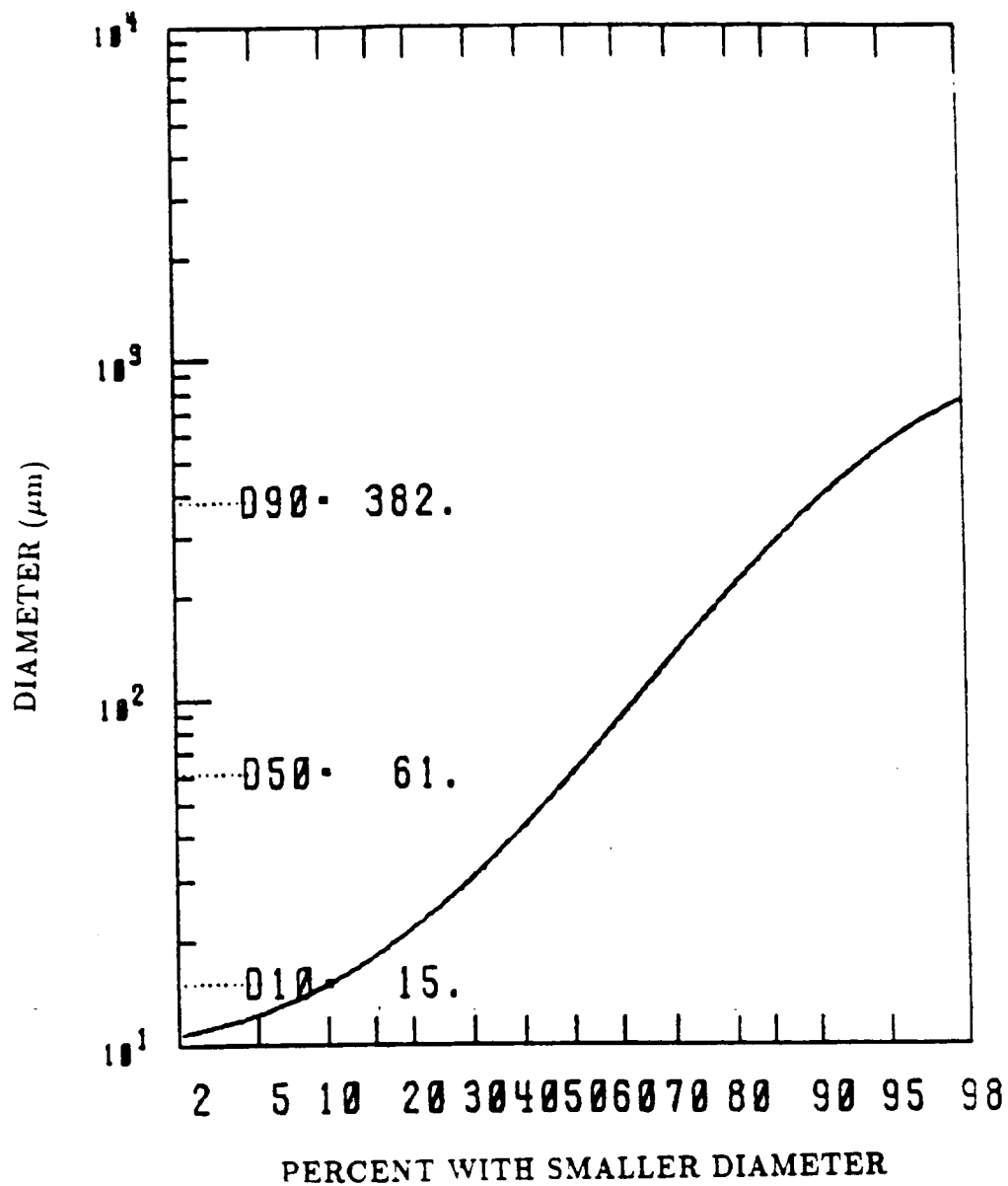
Figure 2.3.12. KDFOC3 Surface-Burst and Base-Surge Activity-Size Distribution. D90, D50, and D10 are the 90th, 50th, and 10th percentile diameter in micrometers, respectively.

Outlines of the effective clouds are shown in Fig. 2.3.2. For the surface burst the activity-size distribution uses the SMALL BOY results. To fit fallout data, however, u_L was changed to 0.2. The stem is tapered from three fireball radii. The radius, top and bottom of the main cloud is given in Figs. 2.3.4 and 2.3.5. The stem cloud radius at its top is one-third the main cloud radius. The taper is a linear interpolation with altitude from the bottom to top. Without the stem cloud and for typical wind and tactical yields, it is obvious from the settling velocity table (See Appendix B) that radioactivity at main cloud heights does not land within one kilometer of ground zero. Close-in activity comes from either the ground zero circle routine or the stem cloud.

The overall vertical distribution of the airborne radioactivity is prescribed by "triangular" distribution functions of altitude: one for the small particles distribution ($k=1$) and a second for the large ($k=2$) particle sizes (for a surface burst see Fig. 2.3.13). Each function, $A_k(h)$, has a mode at h_{mode}, zeros at h_{max} and h_{min} and is normalized so that

$$1.0 = \sum_k \int_{\text{hgz}}^{h_{max}} u_k A_k(h) dh \quad , \tag{2.3.7}$$

where hgz is the altitude at ground zero.

The total airborne radioactivity is then assigned using the total activity-height distribution

$$AHD(h) = \sum_k u_k A_k(h) \tag{2.3.8}$$

for $hgz \leq h \leq hmax$.

As the debris cloud develops, the radioactivity associated with the larger particles leaves the visible debris cloud first, early in the cloud rise episode. The smaller (lighter) radioactive particles rise and stabilize within the main cloud. To incorporate this effect in the cloud-rise model, the mode of the smaller particle activity h_1, is placed at a higher altitude than that for the larger size particles, h_2.
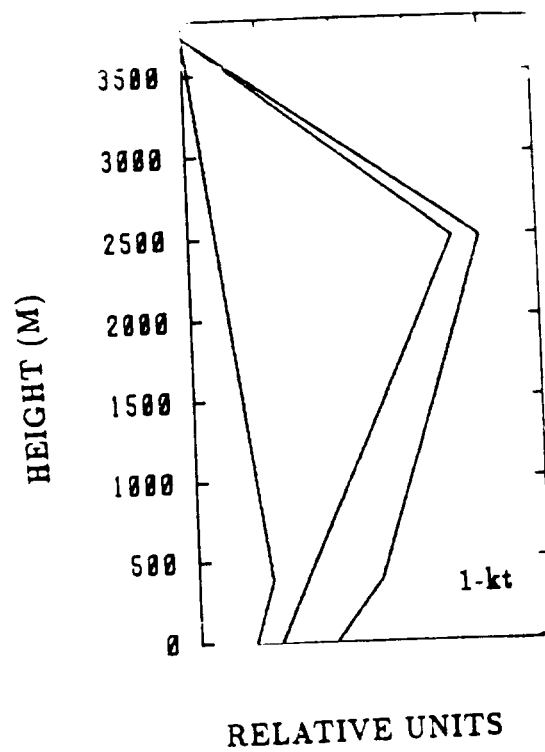
Figure 2.3.13. KDFOC3 Activity-Height Distribution for a Surface Burst.

32

Activity-Altitude-Size Model

The combined activity-altitude-size model can be written as

$$A(h,r) = \sum_k u_k A_k(h) B_k(r) \qquad (2.3.9)$$

for small and large particle sizes.

The rocket probe data of gamma rays taken on the Redwing series indicate substantial radioactivity near the base of the main cloud at 7 minutes and 15 minutes. Thus, we have chosen a peak radioactivity for the small particles at two-thirds the stabilizied height of the top of the main cloud. This is near to the main-cloud base. Because of the structure of near-field fallout patterns, we have adjusted the altitude mode of activity for the larger particles at one-tenth the top of the main cloud.

Especially for buried bursts, the size of the cloud, the amount of radioactivity on the larger particles, and the vent fraction depend strongly on emplacement medium. For example, in dry rock DANNY BOY and CABRIOLET debris clouds are smaller sized and less radioactive than those corresponding to detonations in wet soil. In fact, there was almost no main cloud for dry rock cases.

Hot, wind-influenced patterns around ground zero, however, are similar for both surface and buried explosives. This similarity qualitatively requires a main and tapered stem cloud for each to simulate cloud-rise. For buried detonations massive amounts of crushed overburden smashes back to earth following ejecta deposition. This requires an additional resuspension cloud, the base-surge.

2.4 Transport Model

To evaluate an atmospheric release of radioactivity, its time and scale dependent dilution and transport must be analyzed. The motions and duration of atmospheric turbulent eddies occur over many orders of magnitude. Large scale (synoptic) eddies have horizontal sizes of about 1000 km and last for weeks. Eddy sizes as small as 0.1 cm have lifetimes less than a minute.

The theory of turbulence is based on the concept that turbulent energy is input on the largest size scales, and these large eddies break up into a cascade of smaller eddies, continuing down the size scale until turbulent energy is lost to thermal energy through viscous dissipation. Eddy effects that are larger than grid resolution are modeled by advection, while subgrid eddies are modeled by diffusion. Thus, for our purposes, turbulence is manifested in the random velocity of air (say at a fixed point as a function of time), in contrast to the constancy of steady stream-line flow. Hence, we assume turbulent flow can be resolved into a fluctuating motion superimposed on a mean flow. For a Cartesian coordinate system, the velocity vector is given by

$$\underline{V} = \underline{U} + \underline{u} = \{U_x + u_x, U_y + u_y, U_z + u_z\} \tag{2.4.1}$$

where $\underline{U}$ is the mean flow and $\underline{u}$ is turbulent fluctuation about the mean.

Since we assume we can incorporate subgrid turbulence into a diffusion term, the time dependent, nonlinear convective-diffusion equation of concentration, $\chi(x,y,z,t)$, is given by

$$\frac{\partial \chi(x,y,z,t)}{\partial t} + \underline{\nabla} \cdot [\underline{U}(x,y,z,t)\chi(x,y,z,t))] = \underline{\nabla} \cdot [\underline{K}(t)\underline{\nabla}[\chi(x,y,z,t)]]] \tag{2.4.2}$$

where t is time and $\underline{K}(t)$ is the time-dependent diffusion tensor and $\underline{\nabla}$ is the gradient. If one assumes incompressibility, then $\underline{\nabla} \cdot \underline{U} = 0$ and the transport term becomes $\underline{U} \cdot \underline{\nabla}\chi$.

A convective-size debris cloud grows turbulently from its original size mostly by the influence of similar sized turbulent eddies. Substantially smaller eddies do not separate the cloud sufficiently to cause much growth, whereas substantially larger eddies move the debris cloud as a whole. The effect gives rise to the so-called "scale-dependent diffusion" for large cloud growth.[13]

Settling Speeds

KDFOC3 is a flat terrain "disc tosser" model (see Fig. 2.4.1) that transports each disc in a "Lagrangian" manner with mean wind speeds, $\underline{U}(z)$, specified at heights z above
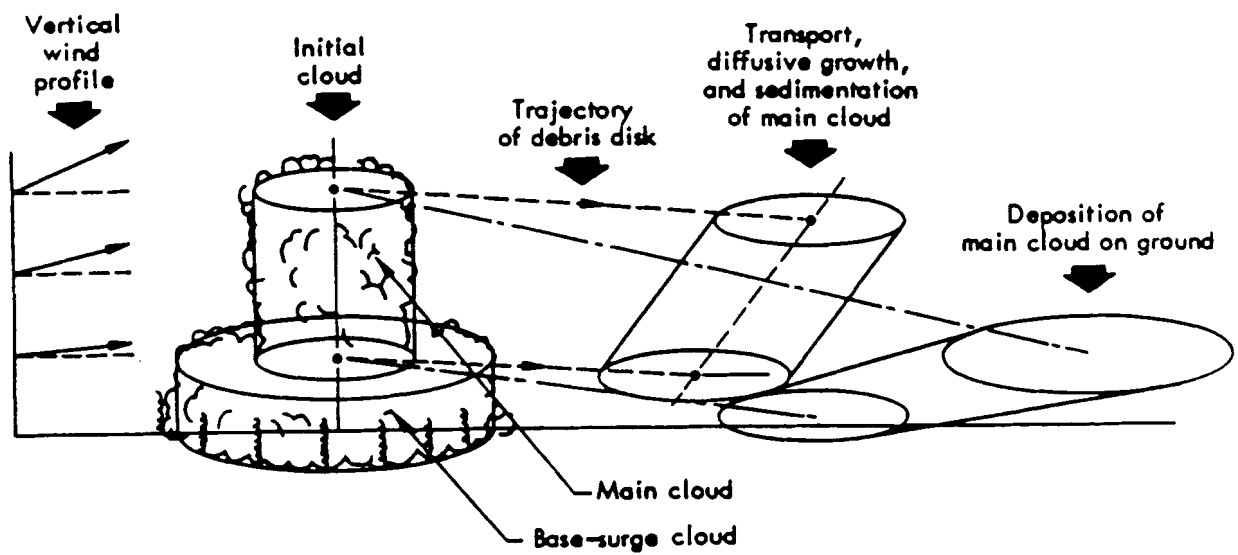
Figure 2.4.1. Schematic of Transport for a "Disc-Tosser" Fallout Model.

ground zero. The vertical transport of each disc is assumed due only to terminal fall speed,
$U_z(r, z) = v(r, z)$, for the particle size r at height z. Thus, the transport part of Eq. 2.4.2
is modeled by

$$x(r, x_o, t) = \int_0^{tf} U_x(z)dt - x_o$$

$$y(r, y_o, t) = \int_0^{tf} U_y(z)dt - y_o \qquad (2.4.3)$$

$$z(r, z_o, t) = z_o - \int_0^{tf} U_z(z)dt$$

for the particle size disc r initially at x_o, y_o, z_o, and for time $t = 0$ to $t = t_f$, the time that
the disc has fallen.

KDFOC3 is a model of local fallout. Substantial particle mass is associated with each
radioactivity particle and causes it to deposit on the ground within the first 24 hours. Very
small particle sizes are ignored. Very large particles fall with a speed so great that they are
not strongly affected by local winds. These are modeled by the ground zero circle routine.

The settling velocity tables (See Appendix B, code listing) are derived from McDonald[14]
data for particles with radii $5 \leq r \leq 500\mu$m, density 2.5 g/cm^3 and for altitudes from sea
level to 50 km.

By assigning each element of radioactivity a size, its settling speed is specified as a
function of altitude. In conjunction with its initial altitude and specified winds, a unique
deposition location is determined.

Diffusion

The diffusion part of Eq. 2.4.2 accounts for growth of discs due to turbulence. We
assume the x and y horizontal diffusion coefficients are equal and the vertical diffusion is
negligible. In fact, the settling speeds of fallout-sized aerosols are greater than vertical
diffusion speeds. Further, upward diffusion would be nearly equal to downward diffusion
if incorporated in the model so that the net effect of discs growing vertically are second-
order effects. Thus, we have found that neglect of vertical diffusion is a good approximation
considering other assumptions and uncertainties within KDFOC3.

The prescription used to describe "scale-dependent" growth is due to Walton.[15]

$$R(t) = R_o \left[1 + \frac{t}{t_o}\right]^{3/2} \quad t < t_2 \tag{2.4.5}$$

$$where \quad t_o = \frac{3}{2} \left[\frac{R_o^2}{\epsilon}\right]^{1/3},$$

$R_o = R(t=0) =$ initial radius of the disk.

$\epsilon = 2.4 \times 10^{-4} \frac{\bar{V}^3}{\bar{z}}$, the energy dissipation rate

$t =$ time for disk to fall to ground

$\bar{V} =$ average wind speed encountered by the disk from its initial

altitude to the surface.

$\bar{z} = 1/2$ distance through which disk falls.

$$t_2 = \left[\sqrt{\frac{2K_{max}t_o}{3R_o^2}} - 1\right] t_o; \quad K_{max} = 7 \times 10^4 \frac{m^2}{sec} \tag{2.4.5}$$

If $t > t_2$, diffusive growth becomes

$$R(t) = \left[R_o^2(1 + \frac{t_2}{t_o})^3 + 2K_{max}(t - t_2)\right]^{1/2} \tag{2.4.6}$$

The "Cloud" Radial Distribution of Radioactivity (ARD)

For each of the cloud discs, the activity radial distribution (ARD) is initially specified by the effective cloud model. Because we have chosen a Fickian-type diffusion model, we assume ARD is initially gaussian about ground zero. The visible cloud radius at stabilization is taken at two standard deviations. Thus, for each disc subdivision in altitude, we define

$$ARD(R, h) = \frac{1}{S(h)(2\pi)^{1/2}} \exp[-1/2(R/S(h))^2] \quad where \tag{2.4.7}$$

$S(h) = 0.5 * R_v(h)$, and R_v is the visible radius of the stabilized cloud at five minutes.

Both the main cloud and the base surge cloud have constant radius from cloud bottom to cloud top (Fig. 2.3.2). The stem cloud is tapered and embedded in the base surge cloud for buried bursts.

The initial diffusion radius is $R_o = R_v$. The transport radius is $R = R(t)$, and is described above. When the disc hits the ground, $R(t)$ and ARD are used to calculate the activity around the landing point.

2.5 Activity Accumulation

One of the important features of KDFOC3 is its method for accumulating radioactivity deposited on the ground. There are several assumptions that are made to make disc summation as simple and fast as possible while conserving radioactivity. These assumptions are:

- the surface is flat;

- the disc is circular;

- a disc's radioactivity arrives simultaneously over its area;

- the radius of each disc, given by Walton's scale-dependent diffusion prescription,[15] contains all the radioactivity;

- the disc is a gaussian, with the radius of the disk equal to two standard deviations; and,

- the center of the disk can be moved to the nearest grid point without introducing significant numerical error into the calculation.

Given these assumptions, the radioactivity is rigorously conserved and only the first disc octant of $\pi/8$ radians needs to be calculated. This substantially reduces computer run time.

We must note here that the last assumption above, i.e., moving the disc centroid to the nearest grid point increases doses along the center-line of the fallout pattern. The smaller the cell size the smaller this effect. Generally, this is a conservative assumption, only slightly increasing doses calculated at each grid point. However, around ground zero, the maximum dose in the pattern can be significantly increased if the grid size is fairly

38

large; thus, the user must be careful in interpreting maximum dose values. They can be quite sensitive to cell size.

The dose rate for a disc at $H + 1$ hour is obtained by summing over

$$d_i(r) = \frac{0.1841 A_i}{\sigma_i^2} e^{-\frac{r^2}{2\sigma_i^2}} \qquad r \leq 2\sigma_i$$

where $\sigma_i = 0.5 R(T_i)$

It is easy to show that

$$A_i = 2\pi \int_0^{2\sigma_i} r d_i dr \ ,$$

where A_i is the fraction of activity that is on the disc, and i represents an element of the set $\{n, m, j\}$, i.e., the cloud, altitude and radius indices associated with each disc in the model (See Section 3.1). For a buried burst there can be up to $3 \times 31 \times 121 = 11253$ discs to consider. Without moving the centroid of the disc to the nearest grid point, certain fallout scenarios can lead to millions of calculations of $d_i(r)$, a formidable numerical task. Using grid symmetries reduces this number by a factor of several.

To calculate estimated doses requires integration of each disc

$$D(r) = \sum_i \int_{T_i}^{TD} d_i(r) t^{-1.2} dt$$

where t is in hours, T_i is the disk deposition time and TD is the departure time of an individual at location r.

If the individual is sheltered, the sheltered dose is given by including a sheltering factor, $s_f \geq 1.0$ in the calculation. Everyone should have a sheltering factor greater than one. An individual in a car or detached home without a basement has a sheltering factor of approximately 2. The dose to a sheltered individual is given by

$$D_s(r) = \frac{D(r)}{s_f} \ .$$

3. USERS MANUAL: INPUT AND ALGORITHMS

Nuclear detonations tend to have the familiar "mushroom cloud" structure. That is, a "main cloud" with a "stem." If the detonation is buried, then there is usually a "base-surge" cloud. Numerical algorithms for KDFOC3, mainly empirically based on the Nevada Test Site series of nuclear detonations, are designed for low-air, surface and sub-surface detonations of nuclear devices from less that 1 ton to 10 Mtons.

Computationally each cloud, $n = 1, N$, is subdivided into MxJ discs for altitude levels hq_m, $m = 1$, M; and particle radii $rp_j, j = 1$, J where M and J are fixed code parameters. Current compilation has M=31 and J=121. The advection due to the wind field, the turbulent diffusion, and the fall time from the stabilization altitude to ground must be computed for each of these discs.

The total fission equivalent yield, wfa, includes the fission products and neutron-induced radioactivity. This is multiplied by a factor vf, which is a product of fractions that determines the amount of airborne activity. This activity is partitioned between discs, then accumulated when it falls to the ground on a numerical x-y grid. The accumulated radioactivity is converted to dose or dose rate by a dose conversion factor for gross fission products, the so-called "dose-area integral". The graphics code (user-supplied) plots contours for final output.

3.1 Preliminaries

In the following sections, code variables will be italicized and subscripts on variables will be array indices with the values:

n=1, ..., $N \leq 3$ for the debris clouds, i.e., main, stem, and base surge
= 1, 2, 3, respectively;

m=1, ..., M   for the altitude subdivisions of each cloud from bottom
to top; and,

j=1,..., J   for the particle size subdivisions from smallest to largest.

40

In the following, res_n are cloud radii at stabilization time, assumed to be 300 seconds. The indices $mc = 1$, $sc = 2$ and $bs = 3$ are specific values of n. We adopt the indexing for types of bursts ($ibtype$):

> Surface or low air burst ($dob=0$ or $hob > 0$, $ibtype=1$) Simulation has main cloud and stem cloud. dob, hob and $sdob$ are depth of burial, height of burst and scaled depth of burial, respectively.

> Deep buried burst ($res_{bs} \geq res_{mc}$, $ibtype=2$) Simulation has main cloud, stem cloud and base surge cloud.

> Shallow buried burst ($sdob < 40$ ft, $ibtype=3$). All three clouds develop. The stem cloud does not "swallow" the base surge.

> Very shallow buried burst ($res_{bs} < res_{sc}$ at top of base surge, $ibtype=4$). A buried burst where the stem cloud "swallows" the base surge. The model has only a main and stem cloud.

Except for a title line and yield, the code is written to provide default values for all parameters not user-specified. Immediately upon execution, the code asks for the name of the input disc file. If the disc file name is "terminal", then the input lines will be requested from the controlling terminal. The "keywords" are read with an a8 format.

The possible input parameters are listed in Table 3.1.1 with their "keywords". Throughout this section mandatory input will be denoted with a superscript**. Optional input will be denoted with a superscript*. This section's description of parameters follows the "keyword" ordering shown. A flowchart and description of code subroutines is given in Appendix B. In this chapter, besides presenting the input parameters, we also discuss the algorithms associated with each.

41

Table 3.1.1: KDFOC3 input variables as described in this section. The keywords "title" and "scenario" are required, and after keyword "scenario," *wtot* is required. All other input is optional.

Key-word	input names, symbols
title	up to 80 alphanumeric characters
scenario	$wtot, pgz$ or $hgz, ffd, inrock, itsdry, dob$ or hob, vf, fv
induced	$wburied, wsurface, wdevice$
gzcirc	$regz, gzexp, gzcon, drgz$
particle	$rbl(2,n), delta(2,n), ul(n)$, for $1 \leq n \leq 3, rmax, rmin$
clouds	$hts(n), hbs(n), res(n)$, for $1 \leq n \leq 3, rfire, rbotsc, sslope, zhat(1),$ $zhat(2), zmax(1), zmax(2), zmin$
winds	$hx(i), th(i), vss(i)$ for $1 \leq i \leq 48$
dose	$dtec, gruff, iwb, shf, tai, tdi, texp, dtable(i)$ for $1 \leq i \leq 5$
grid	$cell, xmin, ymin$
*	end of input this burst, look for another burst
end	end of simulations, terminate

KEYWORD: Title

The "title" line is read with a80 format. The parameters are entered using a fortran NAMELIST format as shown in the sample inputs of Table 3.1.2.

3.2 Scenario

KEYWORD: Scenario

$wtot$** — The total yield [kt] of the device $(10^{-3} \leq wtot \leq 10^4)$. This input is mandatory.

pgz* — Atmospheric pressure [mbar] at ground zero. (Default = 1013.25) hgz and pgz are related by the hh and pl data loaded table values (see section 3.5).

hgz* — Ground zero altitude [m] above mean sea level. (Default = 0.)

Table 3.1.2: Sample KDFOC3 Inputs. The code parameters are italicized here for clarity. Case 1 and 2 describe input for the Cray machine. Case 3 and 4 describe input for the VAX machine. Note the input file is machine dependent.

Case	Input	Comments
1	title 1kt, over land at sea-level scenario $wtot = 1.$ & end	"This case uses all default parameters."
2	title NTS Danny Boy comparison scenario $wtot = 0.42$ $dob = 30.$ $inrock = 1$ $itsdry = 1$ $hgz = 1615$ $fv = 0.6$ & winds $hx(1) = 1615.$ 1669. 1829. 2000. 2134. $th(1)=$ 168. 170. 171. 173. 178. $vss(1) = 6.17$ 6.17 6.71 7.73 7.73 & dose $dtec = 0.75$ $gruff = 0.7$ & end	"Danny Boy comparison at 1615 meters above sea level. D.B was a small yield buried in dry basalt."[16] "We set the dose conversion ($dtec$, $gruff$) parameters for NTS."
3	title 1kt, over land at sea-level scenario &scenario $wtot$=1.0& end	"This case uses all default parameters."
4	title NTS Danny Boy comparison scenario &scenario $wtot = 0.42$ $dob = 30.$ $inrock = 1$ $itsdry = 1$ $hgz = 1615$ $fv = 0.6$& winds &winds $hx(1) = 1615.$ 1669. 1829. 2000. 2134. $th(1)=$ 168. 170. 171. 173. 178. $vss(1) = 6.17$ 6.17 6.71 7.73 7.73& dose &dose $dtec = 0.75$ $gruff = 0.7$& end	"Danny Boy comparison at 1615 meters above sea level. D.B was a small yield buried in dry basalt."[16] "We set the dose conversion ($dtec$, $gruff$) parameters for NTS."

ffd^* — The fission fraction of the device ($0 < ffd \leq 1$). (Default = 1; a fission device).

Not all the radioactivity is lofted on fallout-sized particles. The following input deals with lofted fractions of fallout:

$inrock^*$ — If buried burst ($dob > 0$), and the device is buried in rock, $inrock = 1$. (Default = 0, soil) Cloud dimensions and particle sizes differ depending on the burial medium (soil, wet rock or dry rock)

$itsdry^*$ — If the device is buried in dry rock, then $itsdry = 1$. (Default = 0, wet rock)

dob^* — Depth of burial of device [m]. (Default = 0.) If too deep ($sdob > 200 ft$) for accurate fallout prediction, the code will echo "contained burst". $sdob = dob/0.305 wtot^{0.294} [ft]$. "contained bursts" does not mean that in all circumstances there will be no fallout. We have chosen this cutoff because prediction is unreliable beyond this limit.

hob^* — Height of burst [m]. (Default = 0.) If too high ($hob \geq rb$) for accurate fallout prediction, the code will echo "free-air burst", where $rb = 55 wtot^{0.4}$ [m].

vf^* — Fraction of radioactive material on fallout-sized particles released to the atmosphere. ($vf = fhob * fdry * fsmy * fv$, see below.)

fv^* — Vent fraction is radioactivity on fallout particles. (Default = 0.75)

For $hob \geq rb$ or $sdob > 200$, KDFOC3 estimates no fallout. Otherwise, there are varying amounts depending on conditions. The following parameters are needed to calculate the airborne activity under conditions that have been identified by nuclear testing. The vent fraction for buried bursts is obtained from Fig. 2.2.1. The vent fraction for buried bursts

is reduced if the medium is dry rock. In fact, for *sdob* of about 170 ft, the dry rock vent fraction is about 10% of that for moist rock. We have a linear interpolation on *sdob*. Thus,

$$fdry = \begin{cases} \max\{0.1, 1. - sdob/166.7\} & \text{if } sdob > 0 \text{ and } itsdry=1 \\ 1 & \text{otherwise.} \end{cases}$$

For small devices, *wtot* < 1 kt, observations indicate a reduced amount of radioactivity on fallout-sized particles. We hypothesize that this is due to more rapid cooling, leading to higher supersaturations, thus, more condensation sites and significantly smaller particle sizes. To match the data, we define

$$fsmy = \begin{cases} 1 & \text{if } wtot > 1 \text{ or if } sdob > 15 \\ 1 - (1 - sdob/15)[0.6 - 0.857(wtot^{0.33} - 0.3)], & \text{otherwise.} \end{cases}$$

In the case of the above surface burst, we use a volume fraction that varies from 1 at the surface to 0 when $hob \geq rb$. Thus,

$$fhob = \begin{cases} \frac{(2rb+hob)\ (rb-hob)^2}{2rb^3} & \text{if } 0 \leq hob \leq rb \\ 1. & \text{otherwise.} \end{cases}$$

3.3 Induced Activity

KEYWORD: Induced

If $ffd < 1$ then the induced radioactivity is added and the fission equivalent yield [kt] for a smooth plane is given by

$$wfe = wtot[ffd + (1 - ffd)(wdevice + wsurface + wburied)].$$

where:

*wburied** — A factor [kt fission equivalent yield/kt fusion yield] to give the soil induced radioactivity for buried bursts. (Default = 0.08 min $\{dob, 1\}$).

*wsurface** — A factor [kt fission equivalent yield/kt fusion yield] to give the soil induced radioactivity (Default = 0.08 min $\{1, log(rfire^2 + 1)/log(30^2 + 1)\}$).

*wdevice** — A factor [kt fission equivalent yield/kt fusion yield] to give the device induced radioactivity. (Default $= 0.02$)

The "airborne" fraction of fission equivalent yield [kt] of fission products is

$$wfa = fhob * fdry * fsmy * fv * wfe.$$

3.4 Ground Zero Circle

KEYWORD: Gzcirc

Besides the airborne activity in the fallout clouds, there is activity around ground zero, which accounts for less than five percent of the total activity. To account for the prompt fallout in the immediate neighborhood of the detonation, the following algorithms are used:

*regz** — Radius [m] of pattern at ground zero.

For a surface or low air burst ($sdob=0$)

$$regz = \max\{res_{mc}, 1346wtot^{0.310}\}.$$

For a deep-buried burst

$$regz = res_{bs}.$$

For a shallow-buried burst

$$regz = regz_0 + (res_{mc} - regz_0)(res_{bs}/res_{mc})$$

where

$$regz_0 = \max\{1346wtot^{0.310}, 872wtot^{0.427}\}.$$

*gzexp** — Parameter which determines the exponential falloff of radioactivity in the ground-zero circle of radius of *regz* [m], where

$$gzexp = \begin{cases} 20. & \text{if } sdob=0 \\ 15.3 & \text{if } sdob >10 \\ 20 - 0.47 * sdob & \text{otherwise.} \end{cases}$$

*gzcon** — Ground zero dose rate [rem/hr] for fission device.

$$gzcon = \begin{cases} 2000. & \text{if} \quad sdob = 0 \\ 5000. & \text{if} \quad sdob > 10 \\ 2000. + 300. * sdob & \text{otherwise.} \end{cases}$$

$drgz^*$ — Dose rate [rem/hr at H+1 hr] at device ground zero for thermonuclear

devices ($= gzcon * (wfe/wtot)^{0.629}$).

The ground-zero dose rate over radii, rc, from $rc=0$ to $regz$ is given by

$$drx = drgzx * \exp[gzexp * rc/regz] \qquad \text{where}$$

$drgzx = gzcon * (wfe/wtot)^{0.629}$, and $gzexp$ is given above.

3.5 Activity Size Distributions

KEYWORD: Particle

The total fission equivalent yield, wfa [kt], of airborne radioactivity is in the fallout clouds and on either "large" or "small" particles. Both particle sizes are assumed to be distributed lognormally in particle radius. The distribution of radioactivity with altitude is given by separate triangular functions (Sec. 3.6) for both of the particle sizes. The radioactivity is partitioned to each of the JxMxN discs (J particle radii, M vertical subdivisions, and N clouds: main+stem+possible base surge);

$rbl^*_{k,n}$ — For each cloud, $n=1,N$, the natural logarithm of the geometric mean

radius [μm] for the small ($k=1$), or the large ($k=2$) particle activity

size distribution.

If surface or low air burst, then use activity sizes

$rbl_{1,n}=2.67$,

$rbl_{2,n}=5.02$.

If deep buried, $sdob > 15$, then use activity sizes

$rbl_{1,n}=3.8$,

$rbl_{2,n}=5.7$.

If shallow buried burst, then linearly interpolate using *sdob*

$$rbl_{1,n}=2.67+sdob(3.8\text{-}2.67)/15$$

$$rbl_{2,n}=5.02+sdob(5.7\text{-}5.02)/15.$$

$delta^*_{k,n}$— The natural logarithm of the geometric standard deviation (σ_k) of small ($k=1$), or large ($k=2$) activity size distribution for cloud, $n = 1, N$.

If surface or low air burst, then use

$$delta_{1,n}=1.39$$

$$delta_{2,n}=0.989.$$

If deep buried, *sdob* >15, then use

$$delta_{1,n}=0.7$$

$$delta_{2,n}=0.6.$$

If shallow buried burst, then linearly interpolate

$$delta_{1,n}=1.39+sdob(0.7\text{-}1.39)/15$$

$$delta_{2,n}=0.989+sdob(0.6\text{-}0.989)/15.$$

ul^*_n — For each cloud, $n=1,N$, a partitioning factor for the activity size distributions. ul_n is the fraction put on the larger activity size, and $1\text{-}ul_n$ on the smaller.

If *dob*=0,

$$ul_{mc} = ul_{sc}=0.2,$$

otherwise,

$$ul_{sc} = \min\{0.8, 0.2 + 0.02sdob\}$$

$$ul_{mc} = \begin{array}{ll} \min\{0.5, 0.2 + 0.01sdob\} & \text{if not in dry rock} \\ ul_{sc} & \text{if in dry rock} \end{array}$$

$$ul_{bs} = \begin{array}{ll} 0.2 & \text{if not in dry rock} \\ ul_{sc} & \text{if in dry rock.} \end{array}$$

$rmax^*$ — Radius [μm] of largest size allowed in activity size distribution (500=maximum size in FALLDATA table)

$rmin^*$ — Radius [μm] of smallest size allowed in activity size distribution. (5 = minimum size in FALLDATA table)

Each altitude disc (sec. 3.6) is subdivided into J activity size discs given by

$$rp_j = rmax(rmin/rmax)^{\frac{j-1}{J-1}}, \quad \text{for } j = 1, 2, ..., J.$$

3.6 Stabilized Cloud Description

KEYWORD: Clouds

Determining Cloud Dimensions

We calculate the cloud tops, hts_n, and bottoms, hbs_n, for $hgz = 0$, then we add the surface altitude, hgz. That is, actual cloud height=cloud height given by algorithm + ground height.

Tops of Clouds

hts_n^* — Altitude of top of cloud [meters], for all clouds $n = 1, ..., N$. For all cases, $hts_{sc} = hbs_{mc}$.

If $dob = 0$ (surface burst or above), then (Fig. 2.3.4) applies.

$$hts_{mc} = \begin{cases} 3730 wtot^{0.229} & \text{if} \quad 0 < wtot < 2 \\ 3330 wtot^{0.393} & \text{if} \quad 2 < wtot < 20 \\ 6360 wtot^{0.177} & \text{if} \quad 20 < wtot. \end{cases}$$

If $dob > 0$, then Figs. 2.3.6 and 2.3.8 apply.

For the main cloud, if $ibtype=2$ (deep buried) and not in dry rock, then

$$hts_{mc} = \begin{cases} 3.500(10^3)(0.9918 sdob) wtot^{0.3} & \text{if} \quad sdob \leq 40 \\ 1.828 hts_{bs} & \text{if} \quad 40 < sdob \leq 47 \\ [1.828 + 3.964(10^{-3})(sdob - 47)] hts_{bs} & \text{if} \quad 47 < sdob \end{cases}$$

or, if in dry rock, then

49

$$hts_{mc} = hts_{bs} + 100.$$

For the base-surge cloud, if not in dry rock, then

$$hts_{bs} = wtot^{0.25} \begin{cases} 56.52sdob & \text{if} \quad 0< sdob \leq 20 \\ 1305 + 1.724(sdob - 40) - 0.35(sdob - 40)^2 & 20< sdob <60 \\ (1664 - 7.7443sdob) & 60\leq sdob <200, \end{cases}$$

or, if in dry rock,

$$hts_{bs} = 0.5(hts_{bs} \text{ of not in dry rock}).$$

If $ibtype = 3$ or 4 (shallow or very shallow buried)

$$hts_{mc} = {}^1hts_{mc} * ({}^2hts_{mc}/ {}^1hts_{mc})^{sdob/41} ,$$

preceeding superscripts show interpolation between surface and deep-buried bursts and ${}^2hts_{mc}$ is at $sdob = 41$ m. Let $z_o = hbs_{mc} - (res_{mc} - res_{bs})/slope$, then if $z_o \leq 0$, the stem cloud "swallows" the base-surge cloud and $ibtype = 4$. Otherwise, $ibtype = 3$ and $hts_{bs} = \min\{z_o, {}^2hts_{bs}\}$.

Bottoms of Clouds

hbs_n^* — Altitude of bottom of cloud [m], for all clouds, $n = 1, N$. For all cases, $hbs_{sc} = hbs_{bs} = 0$.

If $dob=0$ (surface or low air burst), then (Fig. 2.3.4)

$$hbs_{mc} = hts_{mc} - \begin{cases} 1740wtot^{0.240} & \text{if} \quad 0< wtot <2 \\ 1720wtot^{0.261} & \text{if} \quad 2\leq wtot \leq 20 \\ 2040wtot^{0.204} & \text{if} \quad 20< wtot. \end{cases}$$

If $dob >0$, then Fig. 2.3.6 applies.

If $ibtype=2$ (deep buried)

$$hbs_{mc} = hts_{bs} .$$

If $ibtype=3$ or 4 (shallow or very shallow buried)

$$hbs_{mc} = {}^1hbs_{mc}({}^2hbs_{mc}/ {}^1hbs_{mc})^{sdob/41}$$

where the pre-superscripts again indicate interpolation between surface and

50

deep buried-burst ($sdob = 41$) values.

Radii of clouds

res_n^* — Radius [m] of cloud at stabilization, $n=1,N$.

If $ibtype=1$ (Fig. 2.3.5 at t=5 minutes),

$$res_{mc} = 872wtot^{0.427}$$

$$res_{sc} = res_{mc}/3 \quad \text{(at stem top)}.$$

If $ibtype >2$ (Fig. 2.3.7 and 2.3.9)

$$res_{mc} = (1 - sdob/210)872wtot^{0.427}.$$

If not in rock ($inrock = 0$), then

$$res_{bs} = wtot^{0.35} \begin{cases} 38.46sdob & 0 \le sdob \le 60 \\ 2690 - 3.22(sdob - 90) - 0.532(sdob - 90)^2 & 60 < sdob < 120 \\ 4836 - 22.68sdob & 120 \le sdob \end{cases}$$

otherwise, if in rock,

$$res_{bs} = (res_{bs} \text{ of not in rock})/3.$$

Radius of Stem Cloud

The radius at the top of the stem cloud is given by

$$res_{sc} = \min\{res_{mc}, res_{bs}/3\}.$$

$rfire^*$ — Fireball radius [m] (Default $= 30wtot^{0.333}$).

$rbot_{sc}^*$ — Multiplicative factor (Default $= 3$) for $rfire$ to determine the radius of the base of the stem cloud.

$sslope^*$ — The slope of the radius as a function of altitude for the tapered stem cloud ($=\max\{0.001, (res_{sc} - rbot_{sc} * rfire)/(hts_{sc} + dob)\}$).

Subdividing into Altitude Discs

Now, having the actual cloud altitudes, each cloud is partitioned into M discs of altitude, each of which will be subdivided to J activity-size discs.

For each cloud $n=1,N$, let

$hq_{1,n} = hbs_n$, the altitude at cloud bottom,

$hq_{M+1,n} = hts_n$, the altitude at cloud top, and

$dhq_n = (hts_n - hbs_n)/\text{M}$.

Then for $m=2,\text{M}$,

$hq_{m,n} = hq_{m-1,n} + dhq_n$.

The "pressure level" subdivisions at the disc bottom are given by

$pq_{m,n} = \text{pf}\ (hq_{m,n})$ for $m = 1,\ \text{M}$,

where pf(h) is an interpolating function.

At this point we have MxJ disks defined for each cloud. We also have the total airborne fission equivalent yield, wfa, in kilotons. This total activity, wfa, is first divided to each cloud, based on the area under two triangular functions of height between the cloud base and the cloud top (see, for example, Fig. 2.3.13). The two functions, AF_1 and AF_2, are defined on the heights using

$zhat_k^*$ — Altitude [m] of peak value of small ($k=1$) or large ($k=2$) activity-size distribution ($zhat_1=(2/3)zmax_1$, $zhat_2=(1/10)zmax_2$).

$zmax_k^*$ — Top [m] of activity-size altitude distributions ($zmax_1=\text{hts}_{mc} - hgz$, $zmax_2 = zmax_1$).

$zmin^*$ — Extrapolated minimum altitude [m] used in computing the vertical distribution of activity ($=-3zhat_2$).

where $zhat_2 < zmax_2 \leq zmax_1 \leq hts_{mc}$, $zhat_1 \leq zhat_2$, and $zhat_1 < zmax_1$. Each triangular function is composed of two linear functions, $f_{k,1}$ and $f_{k,2}$, subject to the conditions that

$$f_{k,1}(zmax_k) = f_{k,2}(zmin) = 0,$$

$$f_{k,1}(zhat_k) = f_{k,2}(zhat_k), \text{ and}$$

$A_{k,1}=$the area under $f_{k,1}$ from $z=0$ to $z = zhat_k$,

$A_{k,2}=$the area under $f_{k,2}$ from $z = zhat_k$ to $zmax_k$,

$$A_{k,1} + A_{k,2}=1.$$

Using the above conditions one derives the function

$$f_k(z) = fzhat_k(z - zmin)/(zhat_k - zmin) \qquad zmin < z < zhat_k,$$

$$f_k(z) = fzhat_k(z - zmax_k)/(zhat_k - zmax_k) \quad zhat_k < z < zmax_k,$$

where

$$fzhat_k = 2(zhat_k - zmin)/[zhat_k zmax_k - zmin(zmax_k + zhat_k)].$$

Since we need the areas under the function $f_k(z)$, we define the area function from altitude base, zb, to top, zt:

$$AF_k(zb, zt) = \begin{cases} 0 & \text{if } zt \leq zmin \text{ or } zb \geq zmax_k, \\ fzhat_k(AF1_k + AF2_k) & \text{otherwise,} \end{cases}$$

where

$$AF1_k = \begin{cases} 0 & \text{if} \quad zb \geq zhat_k \\ (z1 - zb)[0.5(z1 + zb) - zmin]/(zhat_k - zmin) & \text{if} \quad zb < zhat_k \end{cases}$$

with

$$z1 = \min\{zhat_k, zt\},$$

$$AF2_k = \begin{cases} 0 & \text{if} \quad zt \leq zhat_k \\ (z2 - z3)[0.5(z2 + z3) - zmax_k]/(zhat_k - zmax_k) & \text{if} \quad zt > zhat_k \end{cases}$$

with

$$z2 = \min\{zmax_k, zt\},$$

$$z3 = \max\{zhat_k, zb\}.$$

The partitioning of radioactivity to each cloud is given by

$$wac_{k,n} = wfa * AF_k(hbs_n - hgz, hts_n - hgz)(fr_{k,n}/ATOT_k)$$

where $fr_{1,n} = 1 - uln, fr_{2,n} = uln, ATOT_k = \sum_n AF_k(hbs_n - hgz, hts_n - hgz)fr_{k,n}$, for $n=1,N$ (over clouds), $k=1$ for small particle size, $k=2$ for large particle size. Now, each altitude disc ($m = 1,M$) within each cloud ($n=1,N$) and each activity-size disk ($k=1,2$) receives an appropriate amount of radioactivity. Thus we define

$$wad_{m,n,k} = AF_k(hq_{m,n} - hgz, hq_{m+1,n})/AF_k(hq_{1,n} - hgz, hq_{M+1,n}).$$

The final partitioning factor required is over the particle sizes rp_j, $j=1$, J. Let

$$yl_{n,k}(r) = (1/\exp[r])\exp\{-.5[(\ln[r] - rbl_{k,n})/delta_{k,n}]^2\}$$

be the unnormalized lognormal function for particle size k ($=1$, small; $=2$, large) and cloud n. Let

$$fyl_{jn,k} = \int_{r1}^{r2} yl_{n,k}(r)dr / \int_{rmin}^{rmax} yl_{n,k}(r)dr$$

where

$$
\begin{aligned}
r1 &= rmax & &\text{if } j = 1, \\
&= (rp_{j-1}rp_j)^{1/2} & &\text{for } j = 2, J \\
r2 &= rmin & &\text{if } j = J, \\
&= (rp_{j+1}rp_j)^{1/2} & &\text{for } j = 1, J{-}1.
\end{aligned}
$$

The integrations are done numerically using Simpson's rule. Finally, we write the activity assigned to each disc as

$$ar_{j,m,n} = \sum_k wac_{n,k}wad_{m,n,k}fyl_{j,n,k}.$$

3.7 Winds

KEYWORD: Winds

The winds are defined at some number of heights, hx_i [m above mean sea level] for $i=1$, $I\leq48$. If hx_1 is given above the ground, then its corresponding wind vector will also be used at the ground. If the highest wind vector altitude, hx_I, is below the top of the main cloud, then the wind at hx_I will be extrapolated to its top. The centroid of each activity disc, j, will be advected from ground zero (x=y=0) by the x-y velocity components calculated from the input wind vectors, using the degrees clockwise from north, th_i, and wind speed, vss_i interpolated in hx_i to the disc altitude $h_j(t)$ at time t. The user must input all three parameters if the user wants their own winds.

$hx_i{}^*$ — Altitudes of input wind vectors [m] above mean sea level, for $i=1$, $I \leq48$ with $hx_i < hx_{i+1}$.

$th_i{}^*$ — Angle [degrees] from which wind at height hx_i blows, with 0 for wind from north, 90 from east, etc.

vss_i^* — Wind speed [m/s] at altitude hx_i.

If the user supplies the winds, there must be at least one non-zero altitude. For each altitude there must be one wind speed and direction. The number of altitudes, speeds and directions must be the same, and less than or equal to 48 entries. The default wind is a low shear wind with typical speeds that were measured in Germany.[17] It is given by:

hx =1., 500., 1000., 1500., 3150., 5750., 7500., 9500., 10750., 11000., 12250.

th =293., 242., 245., 250., 255., 262., 264., 265., 267., 268., 268.

vss =3.5, 4.5, 6.5, 8.1, 9.9, 13.4, 16.7, 21.1, 21.8, 22.0, 18.4.

The winds are converted to x-y components in the advection calculation as

$$u_k = vss_k \sin(th_k - 180) \qquad \text{[x-direction]}$$

$$v_k = vss_k \cos(th_k - 180) \quad \text{for all heights } hx_k. \quad \text{[x-direction]}$$

Data Tables for Transport

For computation of the fallout pattern, we use the following data (see the code listing in Appendix B for their values):

$$hh_i = 1000\,(i-1),\ i=1,\,27,$$
$$= 2000\,(i-27)+26000,\ i=28,\,39;\ \text{altitudes [m above mean sea level] that}$$
correspond to the pressures, pl_i.

pl_i = pressure [mbar] at altitude hh_i, which is approximately equal to an integration
of the hydrostatic equation with lapse rate of –6°C/km from sea level to
11 km, them zero lapse rate to 25 km, then a lapse rate of 3°C/km to 50 km.
The data are taken from Knox.[12]

$p3_i$, $i = 1,\,12$: pressure levels [mbar] for which particle fall rates are loaded.

rr_j, $j = 1,\,12$; particle radii [μm] for which particle fall rates are loaded.

$Q_{i,j}$ = fall rate [mbar/s] at pressure level $p3_i$ [mbar], $i=1,\,12$; for particles of
density 2.5 g/cm^3 and radii rr_j [μm]; from McDonald.[14]

We assume functions hf(p) and pf(h) are the linear interpolates and inverses between the hh and pl tables. For example, the height above mean sea level of ground zero is

$$hgz = \text{hf}\,(pgz)\ \text{[m]}\ .$$

Advection, Diffusion and Falltime

Given that $p_o > p$, we need to compute the time, $dt_j(p,p_o)$, in seconds for a disc of particle size rp_j to fall from altitude with pressure p to altitude with pressure p_o. Both the particle radius and the pressure levels are linearly interpolated using the fall speed table, $Q_{i,jp}$. For $j = 1$, J and $rr_{jp} \le rp_j < rr_{jp+1}$, let

$$Q'_{i,j} = Q_{i,jp} + (Q_{i,jp+1} - Q_{i,jp})(rp_j - rr_{jp})/(rr_{jp+1} - rr_{jp}),$$
$$b_{i,j} = (Q'_{i+1,j} - Q'_{i,j})/(p3_{i+1} - p3_i)$$

$$a_{i,j} = Q'_{i,j} - p3_i b_{i,j} \quad \text{for } i = 1, 5.$$

Then for $p3_i \geq p_o > p > p3_{i+1}$, the function can be written

$$dt_j(p, p_o) = \int_p^{p_o} \frac{dp}{a_{i,j} + b_{i,j}p} = \frac{1}{b_{i,j}} \ln \left[\frac{a_{i,j} + b_{i,j}p_o}{a_{i,j} + b_{i,j}p} \right] .$$

The wind field is also linearly interpolated in altitude, thus define for $k = 1, K - 1$

$$dudh_k = (u_{k+1} - u_k)/(hx_{k+1} - hx_k) \text{ and}$$

$$dvdh_k = (v_{k+1} - v_k)/(hx_{k+1} - hx_k).$$

Then using the interpolator function hf, $h = \text{hf}(p)$, $h_o = \text{hf}(p_o)$ and for k_p such that, $hx'_{k_p} < h < h_o < hx_{kp+1}$, we write the advection terms for particle size disc j as

$$dx_j(p, p_o) = dt_j(p, p_o) dx dt_j(p, p_o) \text{ and}$$

$$dy_j(p, p_o) = dt_j(p, p_o) dy dt_j(p, p_o) \quad [m]$$

where

$$dx dt_j(p, p_o) = u_{kp} + dudh_{kp}(h' - hx_{kp}), \quad \text{and}$$

$$dy dt_j(p, p_o) = v_{kp} + dvdh_{kp}(h' - hx_{kp}), \quad \text{with} \quad h' = (h + h_o)/2 .$$

We now write the computational algorithms for down time, advection and diffusion of the discs. The procedure is to begin at ground level, then numerically integrate the appropriate values to the next level where either, we reach a disc level, a wind level or a fall-data level for the particular particle size, rp_j. At a fall-data level ($p3$), the i for $a_{i,j}$ and $b_{i,j}$ must be changed. At a wind level hx, the k' for dx and dy must be changed. The Walton[15] diffusion algorithm uses an average wind speed that is independent of particle size; thus, we compute this value to each disc altitude.

At the start of each pressure level we have

$$p_o = p \quad \text{(bottom of current pressure level=top of last level)}$$

$$h_o = h \quad \text{(bottom of current height level=top of last level)}.$$

We compute

$$dtc = dt_j(p, p_o) \text{ [seconds to fall from } p \text{ to } p_o \text{ at bottom of altitude segment]}.$$

For each cloud and each particle size we sum the time it takes for the discs to fall through the levels to the ground,

$$tf_{m,n} \quad = \ tf_{m,n} + dtc \quad [\text{seconds to } pgz \text{ from } p].$$

We also sum the horizontal distances tracked as the disc falls through each wind stratum,

$$xd_{j,m,n} \ = \ xd_{j,m,n} + dxdt_j(p,p_o)dtc \quad [\text{m}]$$

$$yd_{j,m,n} \ = \ yd_{j,m,n} + dydt_j(p,p_o)dtc \quad [\text{m}].$$

If $j=1$ (since average horizontal velocity is independent of j), then

$$ub_{m,n} = ub_{m,n} + (h - h_o)dxdt_j(p,p_o) \quad [\text{m}^2/\text{s}]$$

$$vb_{m,n} = vb_{m,n} + (h - h_o)dydt_j(p,p_o) \quad [\text{m}^2/\text{s}].$$

We now compute the diffusion and the time of arrival of the diffused radiation disc. The initial radius [m] of this disc is its stabilization radius

$$R_o \ = \ res_n \qquad\qquad\qquad \text{if not a stem cloud,}$$

$$= \ res_n + sslope(h - hts_m) \quad \text{if a stem cloud.}$$

The average wind speed to this height is given by

$$sb = \text{sqrt } (ub_{m,n} + vb_{m,n})/(h - hgz)$$

where the atmospheric dissipation rate [m^2/s^3] is defined by,[18]

$$e = (300/z)(sb/5)^3(10^{-4}) \text{ where } z = (h - hgz)/2.$$

Following Walton, we define characteristic times:

$$T_1 = (3/2)(R_o^2/e)^{1/3} \quad \text{and}$$

$$T_2 = T_1\max\{2, [2K_1T_1/(3R_o^2)]^{1/2}\}$$

where T_2 is the time at which the diffused radius is approximately the eddy size at the large end of the inertial subrange and $K_1 = 7 \times 10^4$ m^2/s. If $tf_{m,n} \leq T_2$, then the diffused radius, R is given by

$$R = R_o(1 + tf_{m,n}/T_1)^{3/2} \quad ,$$

otherwise,

$$R = [R_o^2(1 + T_2/T_1)^3 + 2K_1(tf_{m,n} - T_2)]^{1/2}.$$

The diffused radii and downtimes are stored as

$$dfr_{j,m,n} = R \quad [m]$$

$$ttf_{j,m,n} = tf_{m,n} \quad [hrs].$$

3.8 Dose Accumulation Model

KEYWORD: Dose

The accumulation of dose (or dose-rate) on a grid is discussed in this section. Fallout plot routines must be supplied by the user.

In the preceeding sections we have determined for each disc

$xd_{j,m,n}$,	the x-distance from ground zero [m],
$yd_{j,m,n}$,	the y-distance from ground zero [m],
$dfr_{j,m,n}$,	the diffused disc radius [m],
$ttf_{j,m,n}$,	the time from detonation to the arrival of the disc [hr], and
$ar_{j,m,n}$,	the airborne fraction of fission equivalent yield [kt].

for each cloud, $n = 1$, N; for each altitude $m = 1$, M; and for each particle size $j = 1$, J.

Dose Area Integral

Prior to the deposition accumulation of discs, we multiply the disc radioactivity, $ar_{j,m,n}$ [kt], by the dose-area-integral (K-factor),

$$dai = 7.8 \times 10^9 * dtec * gruff \quad [(r - m^2)/(hr - kt) \text{ at 1 hr after detonation}], \text{ where}$$

$dtec^*$ — A factor applied to K of Eq. 2.1.7 to account for detector shielding and efficiency. (Default = 1.0)

$gruff^*$ — A factor to convert from smooth plane dose to real terrain. (Default = 0.7)

59

dai is a dose conversion factor for whole-body gamma radiation from gross fission products at one-hour after detonation. To compare with NTS patterns, *dtec* is about 0.75 and *gruff* is about 0.7. For estimating dose, *dtec* = 1.0 and *gruff* = 0.7, their default values. The total air-borne dose-area integral is obtained by multiplying *wfa* (see Sections 3.2 and 3.3) by *dai*.

Dose Rate

A construct used to compare models with NTS data is the dose-rate calculation for one-hour after detonation. Such a calculation assumes that all the fallout is deposited within sixty minutes of the detonation. When $ar_{j,m,n}$ values and the ground-zero circle calculation are all multiplied by *dai* and summed at a grid point, they give the predicted $H + 1$ hr dose rate, i.e., $drdot = dai * (\sum ar_{j,m,n} + drx)$. To obtain real dose estimates the time of arrival of each disc is considered.

Integrated Dose

iwb^* — A flag to compute dose-rate [rem/hr]. (Default = 0) For integrated dose [rem] use iwb=1.

shf^* — Sheltering factor (inverse of transmission factor). (Default = 1.0)

tai^* — If iwb=1, then *tai* [hrs] is the time an individual arrives in the radiation fallout field. (Default = time activity deposited for each disc)

tdi^* — If iwb=1, integrated whole body dose, then $tdi > tai$ [hrs] is the time an individual departs from the radiation field. (Default = 10^6)

$texp^*$ — If iwb=1, then *texp*. (Default = -1.2) is the radioactive decay constant (must be negative, but not -1). This factor is accurate to about six months.

The integrated whole-body gamma dose is computed by accumulation of

$$shf * drdot \int_{ts}^{tdi} t^{texp} dt$$

60

where *drdot* is the dose rate from either a cloud disc or the ground zero circle at H+1 hours [rem/hr] and $ts=$max{tai, time of disc arrival}.

Both dose and dose rate computations use

*dtable** — Dose or dose rate values of plotted isopleths (to be plotted in user-supplied graphics routine). If dose rates ($iwb=0$), then up to 5 nonzero values [rem/hr at H+1 hrs]. (Default: *dtable* = 10.,30.,100., 300.,1000.) If integrated whole body dose ($iwb=1$) from arrival time (ta) to departure time (td), then up to 5 nonzero values [rem]. (Default: *dtable* = 50., 150., 500., 1500., 5000.)

3.9 Accumulation Grid

KEYWORD: Grid

The accumulation of fallout (deposition) due to the NxMxJ discs is on a finite difference Cartesian (x_i, y_j) grid, $i, k = 1, 2, \ldots,$KP, where x is East and y is North. The burst point is at (x_{ib}, y_{kb}) = (0,0), and is always included in the deposition grid space. The grid is a square one.

*cell** — Grid cell size [m] . $\partial o/ \kappa \ \partial o /$

*xmin** — Minimum value of x [m]. Must be less than 0.

*ymin** — Minimum value of y [m]. Must be less than 0.

The location of the burst point is given by

ib = [$-xmin/cell$] + 1,

kb = [$-ymin/cell$] + 1,

$xmin$ = $-ib(cell)$, and $ymin$ = $-kb(cell)$

so that the burst point (x_{ib}, y_{kb})=(0,0).

If the user does not input the above three values, then the code will derive a relatively optimum grid based on the following algorithms. In this case, the computation time is increased by about a factor of two.

61

The approximate fallout pattern "hot-line" angle is given by the average direction of the advection of main cloud discs. We compute

$$abar = \tan^{-1}(\overline{yd}/\overline{xd})$$

$$\text{where } \overline{yd}_n = \sum_j \sum_m yd_{j,m,n}/jmax * mmax,$$

$$\overline{xd}_n = \sum_j \sum_m xd_{j,m,n}/jmax * mmax,$$

and $n = 1$ for the main cloud.

The estimated length in meters, dwd, of the fallout pattern is based on the empirical equation

$$dwd = 1.3 \times 10^5 \ (dtec * gruff/0.7)(wfa/drmin)^{0.6}, \text{ where}$$

$$drmin = \begin{cases} dtable(1) & \text{if } iwb = 0, \text{ for dose rate, or} \\ dtable(1)/5 & \text{if } iwb = 1, \text{ for integrated dose.} \end{cases}$$

This assumes the lowest dose value of interest is the first entry in $dtable$. To this approximate pattern length we add the "ground zero" circle value or the "base-surge" size at the surface, and compute the grid cell size

$$cell = 1 \cdot 1(dwd * max\{ \mid sin(abar) \mid, \mid cos(abar) \mid\} + radmax)/(KP - 3),$$

where $radmax = max\{regz, res_{bs}\}$, and KP is the (current number) of grid cells.

Having found the approximate pattern length required, and the approximate down-wind direction, we are left to determine the placement of the burst point, (0,0) on the grid. We "off-set" the burst point from the grid edge by a multiple of cell sizes given by

$$ioff = koff = radmax/cell + 1$$

that is, the expected "ground-zero" circle size plus at least three additional cell sizes. We further determine in which sector of the grid we wish to place the burst point, e.g., lower left, lower right, upper left, etc. To this end, we divide the grid into 16 angular sectors each of $\pi/8$ radians, with 0 radians defined as the positive x-axis. We use the wind sector to establish the appropriate burst point on the grid, so that the pattern will not run off the grid and also use essentially the entire grid.

Let $is = abar/(\pi/8) + 1$ (integer value)

and $k35 = 0.35kp$, $k65 = 0.65kp$.

Then set

$ib1 = 1$ if is=1,2,3,14,15,16;

    $= k35$ if is=4,13;

    $= k65$ if is=5,12;

    $= kp$ if is=6, 7, 8, 9, 10, 11; and,

$kb1 = 1$ if is=2,3,4,5,6,7;

    $= k35$ if is=1,8;

    $= k65$ if is=9,16;

    $= kp$ if is=10, 11, 12, 13, 14, 15.

The initial indices for the burst point are given by

ib $= ib1 + ioff + ikoff$ if $ib1 = 1$,

     $= kp - ioff - ikoff$ if $ib1 = kp$,

     $= ib1$ otherwise, and,

kb $= kb1 + koff + kkoff$ if $kb1 = 1$,

     $= kp - koff - kkoff$ if $kb1 = kp$,

     $= kb1$ otherwise.

Finally, the accumulation grid is defined by

$xmin = xp(1) = (1 - ib)cell$

$ymin = yp(1) = (1 - kb)cell$

and the recursive equation of the first paragraph.

If the user has not input the grid using *cell, xmin*, and *ymin*, then KDFOC3 accumulates the deposition, $dep\,(i,k) \geq dtable\,(1)$, on a coarse grid (KP = KG/5) to determine the approximate length and direction of the fallout pattern. If the pattern extends to the grid boundary, then the value for *cell* is increased until the pattern is captured. If less than 1/4

grid length is in pattern, the value of cell is reduced and tried again. Having this position of the deposition pattern, we define a "fine" grid (KP=201) with cell size determined by

$$
cell = \begin{cases} xdir/0.8 * kg & \text{if } xdir > ydir, \\ ydir/0.8 * kg & \text{if } ydir \geq xdir, \end{cases}
$$

where $xdir = xmaxd - xmind$,

and $xmaxd = max \left\{ \mid xp_i - xp_{ib} \mid : dep_{i,k} \right\} > dtable$ (1) for all i, k,

$xmind = min \left\{ \mid yp_k - yp_{kb} \mid : dep_{i,k} > dtable$ (1) for all $i, k, \right\}$ and

$dep_{i,k}$ is the deposition in the cell for (xp, yp) of the coarse grid.

Accumulation Algorithms

The accumulation of activity on the grid is approximated under the assumptions that:

- The activity, $ar_{j,m,n}$, on each disc is represented by a Gaussian distribution with peak value at the disc center, standard deviation of 1/2 of the disc radius. $dfr_{j,m,n}$ and normalized to two standard deviations. A test value,

    $tar = 1.e-6/nmax * jmax * mmax$,

    .has been added. The code will ignore discs with activity less than tar.

- Reasonable accuracy of deposition may be computed by moving the disc center to the nearest deposition grid point and accumulating at all grid cells that intersect the disc. This allows use of grid-point symmetrics when accumulating disc radioactivity which substantially reduces computer costs.

Under these assumptions, for all cloud discs, j=1,J; m=1,M; n=1,N; and the ground zero circle (GZC), the algorithms are:

Locate nearest grid point for each disc centroid;

If GZC, then $id = ib, kd = kb$, the burst point, otherwise,

$$id = xd_{j,m,n}/cell+0.49+bi \qquad \text{if} \quad xd_{j,m,n} \geq 0,$$

$$id = xd_{j,m,n}/cell-0.49+(bi+1) \quad \text{if} \quad xd_{j,m,n} < 0,$$

64

$$kd = yd_{j,m,n}/cell+0.49+bk \qquad \text{if} \quad yd_{j,m,n} \geq 0,$$

$$kd = yd_{j,m,n}/cell-0.49+(bk+1) \quad \text{if} \quad yd_{j,m,n} < 0$$

where bi=float(ib) and bk=float(kb).

Then accumulate at each grid point i, k inside of 2σ such that $1 \leq id + i \leq KP$, and $1 \leq kd + k \leq KP$, with the constraint that $r_{i,k} \leq regz$ if GZC, or $r_{i,k} \leq dfr_{j,m,n}$ if fallout disc $r_{i,k} = cell(i^2 + k^2)^{1/2}$ is the "sampling" radius. We use symmetries to calculate doses in other gradiants.

We define the radioactivity at the sampling radius by:

If in GZC, then

$$rer_{i,k}=\exp[-gzexp(r_{i,k}/regz)] \text{ where}$$

$$gzexp = \begin{cases} \text{input value, or,} & \\ 20 & \text{if } sdob = 0 \\ 15.3 & \text{if } sdob > 10 \\ 20 - 0.47sdob & \text{otherwise.} \end{cases}$$

If a cloud disc, then

$$rer_{i,k}=ar_{j,m,n} \ (0.1841/sig^2)\exp[-0.5(r_{i,k}/sig)^2], \text{ where}$$

$$sig = drf_{j,m,n}/2,$$

and 0.1841 is a factor to normalize the Gaussian figure of revolution to a radius of $2sig$.

Finally, the accumulation for this disc or GZC is completed by

$$dep_{id+i,kd+k} = dep_{id+i,kd+k} + dcf * rer_{i,k} \ .$$

The above computations have produced either an H+1 hour dose rate [rem/hr] (a mathematical construct used to compare with NTS data), or an integrated whole-body dose [rem]. for each cell of the x (East) and y (North) deposition grid, including the activity time of arrival. We now compute some summary information. For each of the dose rate or dose contour table values, $dtable_j$ for j=1, $JD(\leq 5)$ and $0 < dtable_j < dtable_{j+1}$. and using all $1 \leq i, k \leq kp$, let:

$$nc_j = \text{number of cells for which } dep_{i,k} \geq dtable_j$$

where, if the contour level cell count is less than 10 then the dose area is flagged as statistically variable.

To reduce the statistical variation of high dose areas, the area [km^2] enclosed by the dose contour level is approximated by the product of cell area and number of significant cells.

$$ac_j = (cell^2/10^6)nc_j[1 - (nc_j^{1/2}/nc_j)].$$

The "down-wind" fallout pattern (length and direction) for summary information is given by:

$$dxp_j = \max\{|xp_i| \quad : \quad dep_{i,k} \geq dtable_j, \ 1 \leq i,k \leq kp\},$$

$$dyp_j = \max\{|yp_k| \quad : \quad dep_{i,k} \geq dtable_j, \ 1 \leq i,k \leq kp\},$$

$$dwlp_j = (10^{-3})(dxp_j^2 + dyp_j^2)^{1/2} \ [km], \text{ and}$$

$$dwaph_j = 90° - tan^{-1}(dyp_j/dxp_j) \ [\text{degrees from north}].$$

Finally, the maximum dose or dose rate is simply

$$dmax = \max\{dep_{i,k} : 1 < i,k < kp\},$$

which is strongly influenced by the choice of cell size.

3.10   Output

The code produces two output files, namexx.hsp (ascii) and namexx.dmp (binary), where name equals the first seven non-blank characters in title and xx equals 00 - 99. The terminal will give the names of these output files and echo the input filename. Namexx.hsp is the output summary file which gives the physics code output in a readable form, while namexx.dmp is the output dump file feed into the graphics package. The graphics package is not supplied with this code since the graphics are system/package dependent.

Namexx.hsp begins by giving the names of the output summary file, input file, and date and time of run. Following this output is the summarized information of the run, giving the dose rates, areas, down wind distances, angles and cell counts. Then the input

parameters plus some code calculated values are listed by keywords. Last is the name of the output dump file.

Namexx.dmp is a binary write of the commons grafdump and cdose and the values of xp, yp, xmin, ymin, xmax, ymax, cell, dmax, maxd, dwaph, cldsze, dwlp, clcnt, dxp, dyp, and zdcp. The graphics package reads this file and generates a contour plot of the dose rates.

4. REFERENCES AND NOTES

1. Smyth, H.D., 1940: Method of assembly, 12, 19, atomic energy for military purposes. 212.

2. AMBIO, 1982: *A Journal of the Human Environment*, **XI**, number 2–3.

3. Pittock, A.B., T.P. Ackerman, P.J. Crutzen, M.C. MacCracken, C.S. Shapiro, and R.P. Turco, 1986: Environmental consequences of nuclear war—physical and atmospheric effects, Vol. 1.

4. Edwards, L.L., T.F. Harvey, and K.R. Peterson, 1984: GLODEP2: A computer model for estimating Gamma dose due to worldwide fallout of radioactive debris. Lawrence Livermore National Laboratory report UCID-20033.

5. Harvey, T.F., and F.J.D. Serduke, 1979: Fallout model for system studies. Lawrence Livermore National Laboratory report UCRL-52858.

6. Glasstone, S., and P. Dolan, 1977: Effects of nuclear weapons. U.S. Department of Defense.

7. Teller, E., W. Talley, G. Higgins, and G. Johnson, 1968: The constructive use of nuclear explosives. McGraw Hill.

8. This prescription assumes that the half-lives associated with parent-daughter-granddaughter decay chains are such that only one of the half-lives in the chain is commensurate with 10 minute to 50 hour time period. Thus, $a_i(t) = a_i(0)e^{-t/\tau_i}$.

9. Whereas the fission produced radionuclides are only slightly sensitive to the fissile material used, the induced radioactivity is totally dependent on the device construction and device surroundings. The weapon casing and the neutron fluence will change the results for induced activity substantially. Weapons can be designed to enhance or suppress the neutron fluence. Materials can be chosen that when activated result in half-lives which give little radiation in the 10 minutes to 50 hour time frame. The soil constituents and the depth of burial also must be considered in determining the hazardous induced radiation.

10. Dowler, T., August 1975: Private communication, Los Alamos National Laboratory.

11. Harvey, T.F., 1988: Perspective on the local fallout model used in the SCOPE/ ENUWAR STUDY. Lawrence Livermore National Laboratory report UCRL-98589.

12. Knox, J., T. Gibson, and L. Lawson, 1972: private communication.

13. Batchelor, G.K., 1950: The application of the similarity theory of turbulence to atmospheric diffusion. *Quart. J. Ray. Meteor. Soc.,* **76**, 133–146.

14. McDonald, J.E., 1959: Rates of descent of fallout particles from thermonuclear explosions. *J. of Meteorology,* **17**, 380–381.

15. Walton, J.J., 1973: Scale-dependent diffusion. *J. Appl. Meteor.,* **12**, 547.

16. Knox, J.B., 1965: Prediction of fallout from subsurface nuclear detonation. *Proceedings of the Second Conference on Radioactive Fallout from Nuclear Weapon Tests.* Nov. 3–6, 1964, AEC 5 Symposium Series.

17. Peterson, K.R.: private communication.

18. Wilkins, E.M., 1963: Decay rates for turbulent energy throughout the atmosphere. *J. Atmos. Sci.,* **20**, 473–476.

University of California
Lawrence Livermore National Laboratory
Technical Information Department
Livermore, CA 94551